# Water Flow Controls the Spatial Variability of Methane Emissions in a Northern Valley Fen Ecosystem

Hui Zhang[1,2*], Eeva-Stiina Tuittila[3], Aino Korrensalo[3], Aleksi Räsänen[2,4], Tarmo Virtanen[2,4], Mika Aurela[5], Timo Penttilä[6], Tuomas Laurila[5], Stephanie Gerin[5], Viivi Lindholm[4], Annalea Lohila[1,5]

[1]Institute for Atmospheric and Earth System Research (INAR), Department of Physics, P.O. Box 68 (Pietari Kalmin katu 5), University of Helsinki, 00014 Helsinki, Finland

[2]Helsinki Institute of Sustainability Science (HELSUS), 00014 Helsinki, Finland

[3]Peatland and soil ecology research group, School of Forest Sciences, University of Eastern Finland, 8010 Joensuu, Finland

[4]Ecosystems and Environment Research Programme, Faculty of Biological and Environmental Sciences, University of Helsinki, 00014 Helsinki, Finland

[5]Climate System Research, Finnish Meteorological Institute, PL 503, 00101, Helsinki, Finland

[6]Natural Resources Institute Finland, 00790 Helsinki, Finland

*Correspondence to: Hui Zhang (hui.zhang@helsinki.fi)

## Abstract

Northern peatlands are projected to be crucial in future atmospheric methane ($CH_4$) budgets and have a positive feedback on global warming. Fens receive nutrients from catchments via inflowing water and are more sensitive than bogs to climate change-caused variations in their ecohydrology. Yet, due to a lack of data detailing the impacts of moving water on microhabitats and $CH_4$ fluxes in fens, there remains large uncertainties in predicting $CH_4$ emissions from these sites. We measured $CH_4$ fluxes with manual chambers over three growing seasons (2017–2019) at a northern boreal fen. To address the spatial variation at the site where a stream flows through the long and narrow valley fen, we established sample plots at varying distances from the stream. To link the variations in $CH_4$ emissions to environmental controls, we quantified water levels, peat temperature, dissolved oxygen concentration, vegetation composition and leaf area index in combination with flux measurements during the growing season in 2019. We found that due to the flowing water, there was a higher water level, lower peat temperatures, and more oxygen in the peat close to the stream, which also had the highest total leaf area and gross primary production (GPP) values but the lowest $CH_4$ emissions. Further from the stream, the conditions were drier and produced low $CH_4$ emissions. In contrast, $CH_4$ emissions were highest at an intermediate distance from the stream where the oxygen concentration in the surface peat was low but GPP was still high. Our results emphasise the key role of ecohydrology in $CH_4$ dynamics in fens, and for the first time show how a stream controls $CH_4$ emissions in a flow-through fen. As valley fens are common peatland ecosystems from the arctic to the temperate zones, future projections of global $CH_4$ budgets need to take flowing water features into account.

1

# 1 Introduction

Northern peatlands, which cover approximately 15 % of the boreal and arctic regions, are long-term sources of the greenhouse gas methane ($CH_4$) (Korhola et al., 2010; MacDonald et al., 2006), partly counteracting the cooling impact of related long-term carbon dioxide ($CO_2$) uptake. The response of northern peatlands to global warming has partly contributed to the recent increase in atmospheric $CH_4$ concentrations (Bousquet et al., 2011; Ciais et al., 2014; Kirschke et al., 2013), and modelling projections have suggested that, globally, wetland $CH_4$ emissions will continue to increase during the 21$^{st}$ century and have a positive feedback on global warming (Zhang et al., 2017). However, large uncertainties remain in the global $CH_4$ budget models due to limited knowledge of the relative contribution of the various environmental drivers that control $CH_4$ fluxes (Riley et al., 2011). To upscale observed $CH_4$ fluxes and produce realistic scenarios for future projections of atmospheric $CH_4$ concentrations, it is crucial to understand and quantify the correlations between peatland $CH_4$ emissions and their environmental drivers.

In peatlands, $CH_4$ is produced in wet and anoxic conditions below the water level by methanogens, and then released from the peat to the atmosphere. During the transport process, part of the produced $CH_4$ is consumed/oxidised by methanotrophs. The processes of $CH_4$ production, consumption, transport and final release to the atmosphere are affected by several environmental factors, such as water level, organic substrates, and temperature (Abdalla et al., 2016; Bellisario et al., 1999; Larmola et al., 2010). There is also evidence that peatland vascular plant functional types can affect $CH_4$ emissions by altering microbial community structure (Robroek et al., 2015). Sedge-dominated fens are $CH_4$ emission hotspots due to greater methanogenic activity (Juottonen et al., 2005) and better degradation rates (Aerts et al., 1999). Also, the greater abundance of sedges (*Carex* spp.) in fens provides both a direct route for $CH_4$ movement to the atmosphere through aerenchyma tissue, thereby avoiding the oxidation of $CH_4$, and also provides high-quality litter into the soil, which promotes $CH_4$ production (Noyce et al., 2014).

Fens, unlike bogs, are fed by mineral-rich water as seepage from the mineral soil below (soligenous fens) or from surface water flow from the catchment (topogenous fens) (Wheeler and Proctor, 2000). Valley fens that are located in water collecting depressions can receive water from both sources. The spatial variation in the quantity and quality of incoming water creates spatial patterns in vegetation and microbial communities (e.g., methanogens and methanotrophs), and thus $CH_4$ production and oxidation, transportation and ultimately emissions to the atmosphere (Andersen et al., 2011; Juottonen et al., 2015; Kokkonen et al., 2019; Robroek et al., 2015). Several studies have focused on the interactions of $CH_4$ with vertical water level fluctuations. For example, long-term lowering of the water level has been associated with a decreased abundance of *Sphagnum* mosses and aerenchymous plants, decreased $CH_4$ emissions and $CH_4$ production potential (Yrjälä et al., 2011). However, due to the heterogeneity of peatlands, inconsistent patterns can also be found. For instance, several studies have indicated that greater $CH_4$ emissions occur when the water level is close to the surface of the peatland (Bubier et al., 2005; Pelletier et al., 2007), while other studies have found maximum fluxes occurred at intermediate water levels (Turetsky et al., 2014), or found no connection between $CH_4$ emissions and water level (Euskirchen et al., 2019, Korrensalo et al., 2018). Nevertheless, water level has been suggested as a more important forcing factor on $CH_4$ cycling in fens than either

temperature or vegetation composition alone (Laine et al., 2019; Mäkiranta et al., 2018; Riutta et al., 2020). In addition to vertical water level changes, the lateral flow of water in fens can be even more important in driving the processes that underpin $CH_4$ emissions, because flowing water not only ensures a water supply for the vegetation, but also transports nutrients, which benefits vegetation and microbial communities (Laitinen et al., 2007). At the same time, flowing water is likely to transport more oxygen (Ingram, 1983), thus enhancing $CH_4$ oxidation and suppressing production. While fens are typically the highest $CH_4$ emitters of all peatlands (Turetsky et al., 2014), the influence of lateral water flow on fen $CH_4$ emissions has not been studied to date.

At a global scale, climate warming is projected to continue in the decades ahead, while changes in precipitation patterns are projected to be more regional (Collins et al., 2013). The Coupled Model Intercomparison Project (CMIP5), under a RCP8.5 scenario, predicts a warmer and wetter climate for Fennoscandia (Collins et al., 2013). As peatland hydrology is driven by several processes, such as precipitation, lateral water fluxes, transpiration and evaporation, climate model predictions cannot be directly applied to infer peatland hydrological conditions (Helbig et al., 2020; Tuittila et al., 2007; Wu et al., 2010; Zhang et al., 2018), especially in minerotrophic fens. Nevertheless, peatland habitats can be impacted under both warming-dry and warming-wet scenarios (Bjorkman et al., 2018; Strack et al., 2006). In addition, fens may be more sensitive to water level changes than bogs; in particular, their plant communities have been shown to experience clear species turnover under drier conditions (Kokkonen et al., 2019). Aside from the vertical fluctuations in the water level, climate change is also likely to affect the water that enters fens as it will control the hydrological conditions within the catchments, e.g., the temperature sum in spring strongly controls the timing and amount of snowmelt water that enters the fen. This type of change in catchment conditions is likely to impact, for example, plant phenology and biomass production (Mäkiranta et al., 2018). This will, in turn, impact on C cycling between the peatland and the atmosphere due to different photosynthesis, decomposition and gas transportation rates, and on other factors at the plant functional type and even at the species levels (Hajek et al., 2009; Laine et al., 2011; Turetsky et al., 2008). Hence, a full insight into the complex climate-peatland-ecohydrology-$CH_4$ relationship is needed to predict the impact of changing catchment hydrology on fen $CH_4$ emissions under climate change scenarios. Prior to importing peatland-scale $CH_4$ emissions into global circulation models, we first need to bridge the gap of understanding as to how water flows control fen microhabitats and $CH_4$ emissions.

In this study, we aimed to assess the role of flowing water in regulating spatial variations in valley fen vegetation and $CH_4$ emissions. More specifically, we asked the following research questions: 1) How does a flowing stream within a valley fen impact microhabitat conditions, vegetation composition and biomass production? 2) Does the distance to a stream modify $CH_4$ fluxes? 3) How does vegetation composition and stream-related variables control $CH_4$ emissions? We hypothesised that: (H1) water table, temperature, oxygen concentration, vegetation structure and biomass are related to the proximity of the stream; (H2) spatial variation in $CH_4$ fluxes is related to the distance from the stream; (H3) regulation of $CH_4$ fluxes by the stream is mediated by the vegetation and by environmental variables, such as oxygen concentration.

## 2 Material and methods

## 2.1 Study site

Lompolojänkkä (67.997 °N, 24.210 °E, 269 m a.s.l.) is one of the Finnish Integrated Carbon Observation System (ICOS) sites. It is an open mesotrophic sedge fen that is located in a valley in the hilly Pallas region of northern Finland (Figure 1). Based on the 30-year average (1981–2010; Kittilä Pokka meteorological station), the annual average temperature and total precipitation are -1.3 °C and 547 mm, respectively (Pirinen et al., 2012).

105
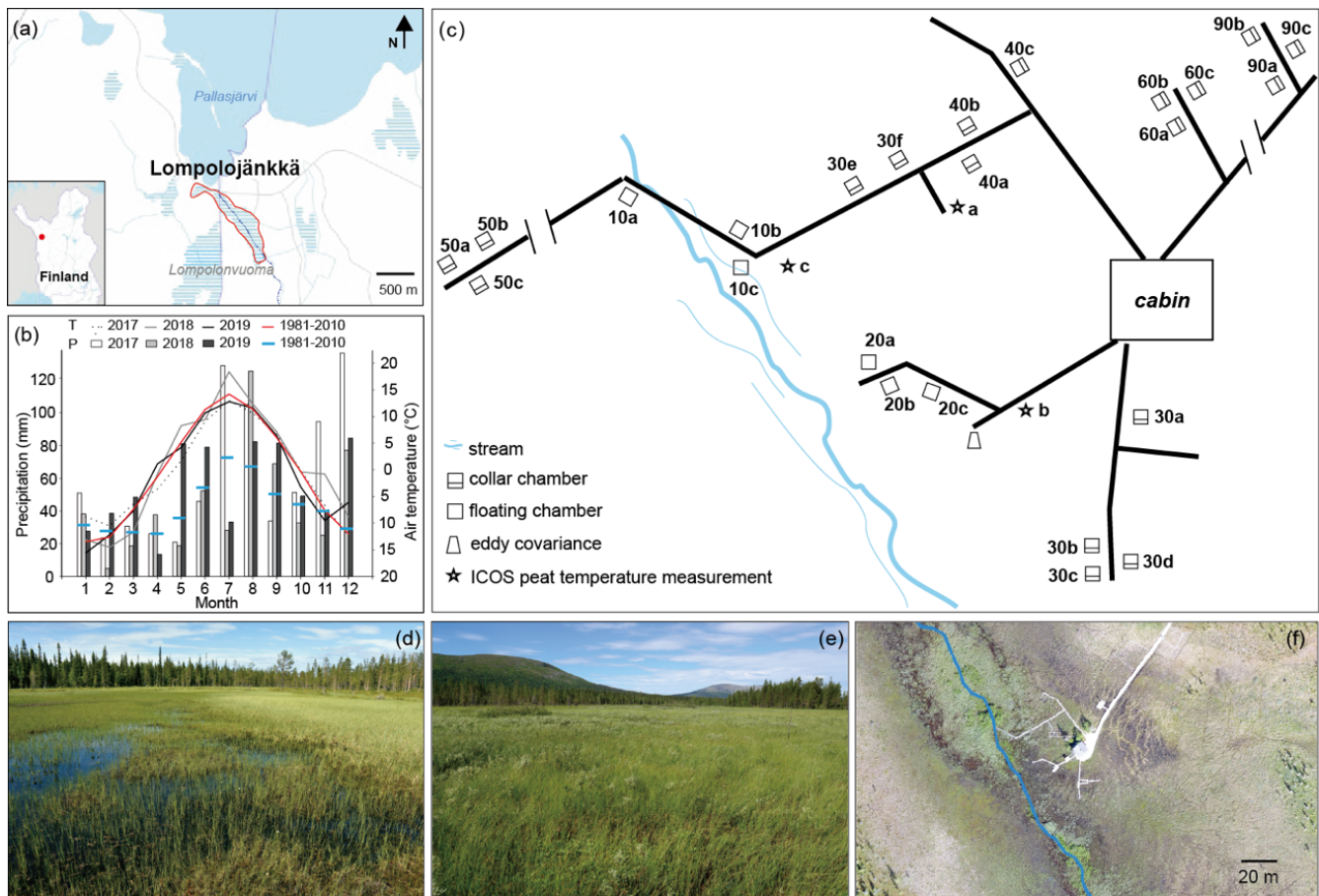


**Figure 1:** (a) Location of the Lompolojänkkä study site outlined in red, with the stream marked in blue. The base map was downloaded from the National Land Survey of Finland dataset under a CC 4.0 open source license. (b) Monthly air temperature (T) and precipitation (P) during 2017–2019, and long-term mean T and P values (1981–2010; Kittilä Pokka meteorological station https://en.ilmatieteenlaitos.fi/statistics-from-1961-onwards). The data for 2017–2019 were obtained from the nearest meteorological stations; Lompolonvuoma (for temperature) and Kenttä (for precipitation) (https://en.Ilmatietee nlaitos.fi/download-observations#!/). (c) Schematic illustration of the field measurement setup. (d, e) Photos of the study site. (f) Drone image of the field measurement area with the stream indicated in blu

4

During the three flux measurement years (2017–2019), the summer of 2018 was exceptionally warm, up to 5 °C warmer than the long-term average (Figure 1b). Based on the ICOS continuous peat profile temperature measurements (at 5, 10, 20, 30, 50 and 100 cm; Figure 1c) in 2018, peat temperature at Lompolojänkkä varied along depth and also for different habitats (Figure A1). During summer, peat temperature decreased from the surface to the deeper layers and the pattern was reversed for the other seasons. Peat temperatures were greater in the drier parts of the study site compared to the wetter parts (closer to the stream) at all measured depths, and there were also larger temperature variations between the different depths.

Peat accumulation at Lompolojänkkä initiated around 10,000 cal. yr BP (calibrated years before the present 1950 AD) and the deepest peat depth is approximately 2.5 m (Mathijssen et al., 2014). Almost the whole peatland is water saturated throughout the year. The relatively dense vegetation layer is dominated by different sedges (e.g., *C. rostrata*, *C. chordorrhiza*) in the wet areas and various deciduous shrubs (e.g., *Betula nana*, *Salix phylicifolia*) in the relatively dry areas. Moss cover (e.g., *Sphagnum* spp.) is patchy with *c.* 70 %-cover (Aurela et al., 2009). A small stream flows through the long and narrow valley fen (outlined in Figure 1a) and empties into the nearby Pallasjärvi lake. The flow and size of the stream varies seasonally; being largest in spring after snow melt in the catchment. During summer, the stream water level in many locations is below the vegetation surface and may not be visible (Figure 1d). For more detailed descriptions of Lompolojänkkä, see Aurela et al. (2009) and Lohila et al. (2010).

## 2.2 Sampling / sample plot set up

To quantify the spatial variability in $CH_4$ fluxes in the valley fen, we installed 15 permanent sample plots 60 cm x 60 cm (W x L) at varying distances from the stream in 2017 (Table 1). The sample plots were set up as clusters of three to six plots that were typically located within a metre of each other. Initially, the closest cluster from the stream was located within a 10-m distance, and the furthermost at a 40-m distance. In 2019, we sought a better mechanistic understanding of the controls on $CH_4$ fluxes and so we added nine more sample plots, located in three clusters at 50, 60 and 90 m distance from the stream (Table 1).

**Table 1:** Methane ($CH_4$) flux sample plot setup and measured variables at Lompolojänkkä. DTS: distance to stream; PCT: plant community type; $T_{air}$: air temperature; T5: peat temperature at depth 5 cm below moss surface; WT: water table; DO20 and DO40: dissolved oxygen concentration at 20 and 40 cm below the peat surface; LAI: leaf area index.

| Year | No. of plots | Plot codes | Measured environmental variables |
|------|-------------|-----------|----------------------------------|
| 2017 | 15 | 10a-c, 20a-c, 30a-f, 40a-c | DTS, PCT, $T_{air}$ |
| 2018 | 15 | 10a-c, 20a-c, 30a-f, 40a-c | DTS, PCT, $T_{air}$ |
| 2019 | 24 | 10a-c, 20a-c, 30a-f, 40a-c, 50a-c, 60a-c, 90a-c | DTS, PCT, $T_{air}$, T5, WT, DO20, DO40, LAI |

In total, 24 permanent gas flux measurement plots were established (Table 1, Figure 1c). The sample plots are coded according to their distance to the stream/visible flowing water as 10a-c (a cluster within 10 m to the stream with three replicates a-c), 20a-c, 30a-f, 40a-c, 50a-c, 60a-c and 90a-c. The location of each plot was measured with a Trimble R8 GPS device with ±5 cm accuracy and the distance to the stream from each sample plot was calculated based on the National Land Survey of Finland topographic database.

## 2.3 $CH_4$ and $CO_2$ flux measurements

Seasonal $CH_4$ and $CO_2$ (dark respiration) fluxes were measured for three years (2017–2019) in sample plot clusters 10–40, and for one year (2019) in series 50–90. Measurements at clusters 10–40 were conducted eight times in 2017 (between 13 June–29 September), 11 times in 2018 (between 30 May–11 October) and 15 times in 2019 (between 20 May–11 September). At clusters 50 and 90, measurements were conducted 11 times in 2019, and 21 measurements were performed at cluster 60. In total, these measurements yielded 126, 163 and 330 $CH_4$ flux records for 2017, 2018 and 2019, respectively.

For determining fluxes, the closed chamber method with fixed collars was used for clusters 30–90, and a floating chamber method without collars was employed for clusters 10 and 20 (Alm et al., 2007). The size of the opaque aluminium chamber was 60 cm x 60 cm x 40 cm (W x L x H) and each chamber was equipped with a fan. The sample gas was sucked from the chamber at a flow rate of 200–200 ml min$^{-1}$ using 50-m long tubing (d=6 mm) into a LGR gas analyser (LGR GCA-24p-EP, model 911-0011-0004, Los Gatos Research Inc., Ca, USA) located in a temperature-controlled cabin. The duration of one measurement was approximately 5 mins. The floating chamber (60 cm x 60 cm x 30 cm) was used at plots with permanently high, flowing water. In addition, gross primary production (GPP) was measured at clusters 10–40 using a transparent chamber on 24–25 July 2019 at the time of peak growing season. Same gas analyser as described above was used. Photosynthetically active radiation in the chamber was measured using a Kipp&Zonen PQS1 PAR Quantum Sensor (Kipp & Zonen B.V., Delft, the Netherlands). In order to fit a light-response curve to the net $CO_2$ exchange (NEE) data, NEE was first measured in full light, after which the chamber was covered with fabrics to create four different light levels (white shade, black shade, double black shade, and double black with green shade). In addition, one measurement with full shading to capture dark respiration was performed.

The $CH_4$ and $CO_2$ fluxes from each measurement were calculated from the linear slope ($R^2 > 99$ % for over 90 % measurements and $R^2 > 90$ % for other measurements) in gas concentration over time, taking into account chamber volume, chamber air temperature and air pressure at the measuring point. The volume in the chamber during each measurement was specified according to the instant ambient water level. The air temperature and air pressure data were derived from the nearest meteorological station, and air pressure was calibrated for each chamber, taking into account the altitude of the plot. We determined the GPP-light response curve for each sample plot (based on the NEE measurements with the transparent chamber), and derived sample plot specific GPP$_{max}$ values at a photosynthetic photon flux density level of 800 µmol m$^{-2}$ s$^{-1}$.

**2.4 Environmental data collection**

To reach a mechanistic understanding of the spatial pattern of $CH_4$ fluxes, we collected data on the potential environmental
factors that control emissions in combination with each flux measurement conducted in 2019. These factors were air and
peat temperature, water table, dissolved oxygen concentration, leaf area index, and plant community cluster (Table 1).

Air temperature was either measured using a temperature sensor fixed inside the chamber or measured at 2-m height at the
site (Lompolonvuoma meteorological station of Finnish Meteorological Institute (FMI)). Peat temperature was measured at 5
cm below the moss surface (T5) using a Pt100 thermometer (Omega HH376, Omega Engineering Inc., CT, USA). Water
table relative to the moss surface (WT) was measured from a plastic tube installed in the peat next to each sample plot.
Dissolved oxygen concentration 20 (DO20) and 40 cm (DO40) below the surface (except cluster series 60) were
measured using a YSI Professional Series Digital handheld meter.

The leaf area index (LAI) of four vascular plant functional types (PFTs; deciduous shrub, evergreen shrub, forb and
graminoid), and moss cover were estimated. The estimation of LAI followed Juutinen et al. (2017). First, we selected 31
square plots (50 cm × 50 cm) located within the fen and surrounding areas in July–August 2019, and estimated green
projection cover (%) and measured mean height for each PFT in the plots. Second, to measure LAI of the samples, we
harvested the aboveground parts of the vascular plant species, scanned them with an A4 scanner and calculated the
proportion of green pixels in GIMP 2.8 (The GIMP Team, www.gimp.org). Third, we constructed empirical relationships
between cover or plant volume (cover × height) and LAI with ordinary least squares (OLS) regressions for four PFTs found
in the site. We chose the optimal predictor (cover or volume) by minimising the root mean square error value, and in the
final models, the adjusted coefficient of determination (Adj.$R^2$) varied between 0.73 and 0.89 (Table A1). Fourth, we used
the equations from the OLS regressions to model seasonal LAI development curves for each $CH_4$ sample plot in which we
had measured green projection cover and height for the four PFTs throughout the summer of 2019. Finally, we derived LAI
values for each flux measurement time from the seasonal LAI development curves. We also calculated LAI values for the
aerenchymous plants in each plot, which included *C. aquatilis*, *C. canescens*, *C. chordorrhiza*, *C. lasiocarpa*, *C. limosa*, *C.
rostrata*, *Comarum palustre*, *Equisetum fluviatile*, *Eriophorum vaginatum*, and *Menyanthes trifoliata*. The calculation of
aerenchymous LAI was carried out by applying the same OLS regression equations used for forb and graminoid PFTs to
datasets that included only aerenchymous plant species.

In addition, we delineated four plant community types/clusters for the $CH_4$ sample plots as follows. First, we calculated the
Bray-Curtis distance matrix of the plant species projection cover data from the sample plots and, in addition, 200
systematically sampled vegetation plots that were inventoried in the fen in 2018. Second, we derived four non-metric
multidimensional scaling ordination (NMDS) axes from the distance matrix. Third, we delineated four plant community
clusters from the NMDS axes with the Partitioning Around Medoids (PAM) method. The clustering was conducted in R with
packages 'vegan' (Oksanen et al., 2019) and 'cluster' (Maechler et al., 2019). A map showing the location of the vegetation
community clusters in the study site can be found in Figure A2.

## 2.5 Data analysis

NMDS was used to explore the linkages between peak season vegetation composition, distance to the stream, biomass production and flowing water. Peak season total LAI was used as a proxy for biomass production, and early summer DO20 and DO40 were used as proxies for flowing water/nutrient availability. For a robust analysis, plant species with occurrence lower than 3 % were excluded from the analysis.

Linear mixed-effect models were applied to the $CH_4$ flux and environmental data to identify the potential drivers of $CH_4$ flux using two different approaches. First, we explored the spatial variation in $CH_4$ fluxes by constructing a model with $CH_4$ data from all three measured years. Here, potential fixed predictors for $CH_4$ flux were distance to the stream, air temperature and the factorial plant community cluster. To account for repeated measurements, we included the nested random effects of year, month and measurement plot. Second, to gain a mechanistic understanding of the controls on $CH_4$ fluxes, we used a dataset with additional variables gathered during 2019. Here, potential fixed predictors were DO20, DO40, T5, air temperature, WT, $GPP_{max}$, LAI of all vascular, aerenchymous and ericoid plants, moss cover (% coverage), $CO_2$ dark respiration, distance to the stream, and the factorial plant community cluster. To account for repeated measurements from the plots over the growing season, we included the crossed random effects of measurement day and plot.

In building the models, we manually added the potential fixed predictors one by one and tested whether the resultant, more complex model was significantly better than the model without the added predictor, using conditional *F*-test and Akaike information criterion (AIC). To account for the nonlinear relationship between $CH_4$ flux and some environmental variables (such as temperature), we tested several response shapes for the fixed predictors: i) linear response, ii) quadratic response, iii) linear response above or below a certain threshold value, but constant otherwise, and iv) quadratic response above or below a certain threshold value, but constant otherwise. In cases iii) and iv), the response type and threshold value were determined visually by plotting the residuals of the previous model against the fixed predictor to be added. The final response shape and threshold value were selected based on the conditional *F*-test and AIC values. Furthermore, we tested the interactions between all fixed predictors in the final models and only included those predictors that led to a significant improvement in model performance. The first explorative model was fitted with function lme of the package 'nlme', and the second more complex mechanistical model was fitted with function lmer of the package 'lme4' in R.

## 3 Results

### 3.1 Variations in vegetation and environmental factors

The studied valley fen exhibited clear but distinctive patterns in vegetation composition, WT, LAI, and DO concentrations related to distance from the stream (Figures 2 and A2–5). Moreover, the temporal patterns in WT and DO concentration showed distinct variations at locations further away and closer to the stream, respectively (Figure A4).

In total, four plant community types were identified (Figure 3, Table A2). Community type (1) fluvial, which was found in the wetter parts of the fen, was dominated by *E. fluviatile* and *C. limosa*. Community type (2) riparian represented riparian vegetation that were taller, such as *C. aquatilis*, *S. lapponum*, *S. phylicifolica* and *Comarum palustre*. Community type (3) lawn, and community type (4) hummock contained vegetation typical of drier fen conditions, with the hummock type found in the driest areas. The dominant species in these community types included *S. riparium*, *Vaccinium oxycoccos* and *C. livida* (lawn), and *S. russowii*, *V. uliginosum*, *Betula nana* and *Rubus chamaemorus* (hummock). The overriding pattern was related to the distance to the stream (Figure 2a and A2), i.e. fluvial and riparian community types were recorded in the locations closest to the stream, while lawn and hummock types were located at the plots furthest from the stream. In addition, the plant communities in the sample plots were suggestive of a spatially heterogeneous structure in the fen, i.e. different types were recorded within a short distance (Figures 2a and 3). The NMDS ordination (Figure 3) revealed that the main pattern in vegetation structure related to the distance to the stream was correlated strongly with, and was better explained by, peak season oxygen concentration. Total LAI increased with peak season oxygen concentration, which was negatively correlated with distance. Aquatic species, such as *C. aquatilis* and species that typically benefit from moving water, such as *S. lapponum*, *C. palustre* and *M. trifoliata*, exhibited relatively high positive values on the first NMDS axis, revealing a strong relationship between the stream and some specific plant species. Species adapted to drier surfaces, such as mosses *Rhizomnium* sp. and *S. warnsdorfii* and the sedge *E. vaginatum*, were located at the other end of the axis. As peak season GPP data were only available for clusters 10–40, they were not included in the NMDS analysis, but were analysed separately against oxygen concentration and total vascular LAI data (Figure A6). GPP was clearly higher closer to the stream ($> 0.45$ mg $CO_2$ m$^{-2}$ s$^{-1}$) than further from the stream ($< 0.35$ mg $CO_2$ m$^{-2}$ s$^{-1}$). In addition, GPP was strongly related to total vascular LAI, at least when LAI $< 2$. In the only sampling point with a LAI value $> 2$, GPP did not increase any further.

The WT pattern at the sample plots was strongly linked to their distance to the stream, i.e. WT was higher closer to the stream (Figure 2b). At clusters 10 and 20, close to the stream, there was approximately 10 cm of water above the peat surface, while at cluster 90, furthest from the stream, the WT was approximately 10 cm below the surface. The other clusters displayed intermediate WT values. In general, the lowest (deepest) WT levels were measured at all sample plots during late July, when precipitation was low and air temperature had reached the seasonal peak (Figures A4 and A7).

The sample plots located next to the stream (cluster 10) showed significantly larger mean seasonal vascular LAI values (mean 1.5) but were similar to cluster 60 (with lawn vegetation) (Figure 2ac). Clusters 10 and 60 both showed significantly higher aerenchymous LAI values than the other clusters (~0.5), although cluster 10 (mean 1.4) had a significantly higher value than cluster 60 (mean 1.1) (Figure 2c). Plot 10a appeared to be an outlier with higher total and aerenchymous LAI values (~4) than the other plots ($< 2$), which was attributed to the presence of the abundant forb *C. palustre* in that plot (Figure A3). Graminoid LAI values (that excluded *C. palustre* and two other occasionally recorded species: *M. trifoliata* and *E. fluviatile*) were significantly higher in cluster 60 (mean 0.8) than in the other clusters ($< 0.5$). The development of LAI showed a clear seasonal pattern (Figure A5), with the peak occurring around late July.

270 Dissolved oxygen concentrations at both 20 and 40 cm depths showed a similar spatial pattern, with higher concentrations recorded close to the stream (in clusters 10 and 20) (Figure 2d). However, large temporal variations existed in DO values at both the 20 and 40 cm depths, which generally peaked in early summer during a high flow of water (Figure A4). Also, DO concentrations showed a similar temporal pattern to precipitation, with higher concentrations recorded during periods with higher precipitation (Figures A4 and A7).

275 The proximity of the stream reduced the temporal variation in the peat temperature measured at 5 cm depth in 2019 (Figure A4); while the temperature at sample plots further away (clusters 50–90) varied between 3 and 23 °C, and the temperature at sample plots close to the stream (clusters 10–40) stayed between 7 and 15 °C.
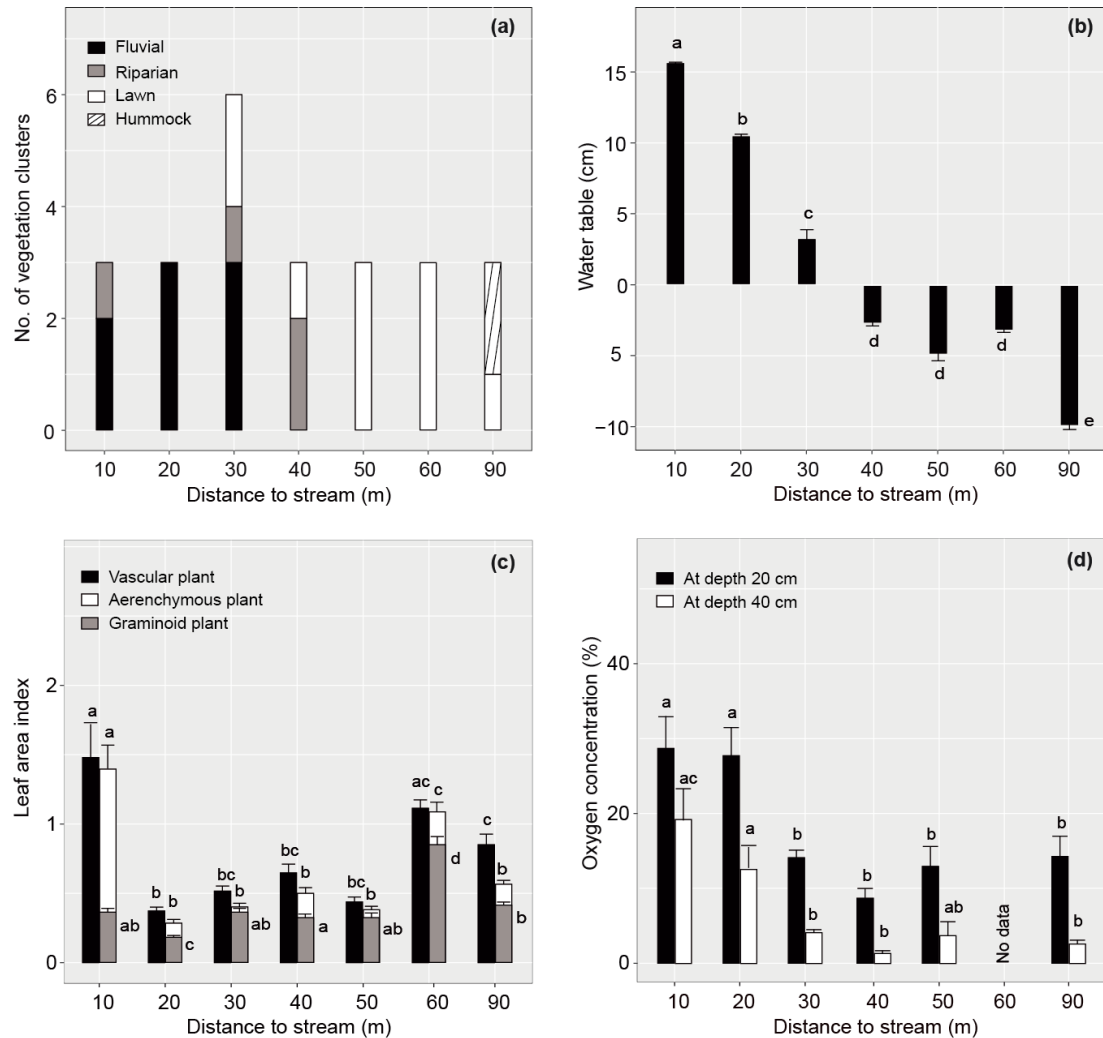


280 **Figure 2:** Spatial variation in vegetation and environmental factors in relation to the distance of the sample plot cluster from the stream in summer 2019. (a) Occurrence of different plant community types, (b) mean (± standard error) water table relative to peat surface (cm), (c)

vascular, aerenchymous and graminoid plant leaf area index, and (d) dissolved oxygen concentration at 20 and 40 cm below the peat surface for each sample plot cluster. Note that dissolved oxygen concentration was not measured at cluster 60. Different letters above the bars indicate significant differences ($p < 0.05$) between the sample plot clusters calculated using Tukey's Honest Significant Difference method. For species composition in the different plant community types, see Figure 3 and Table A2.
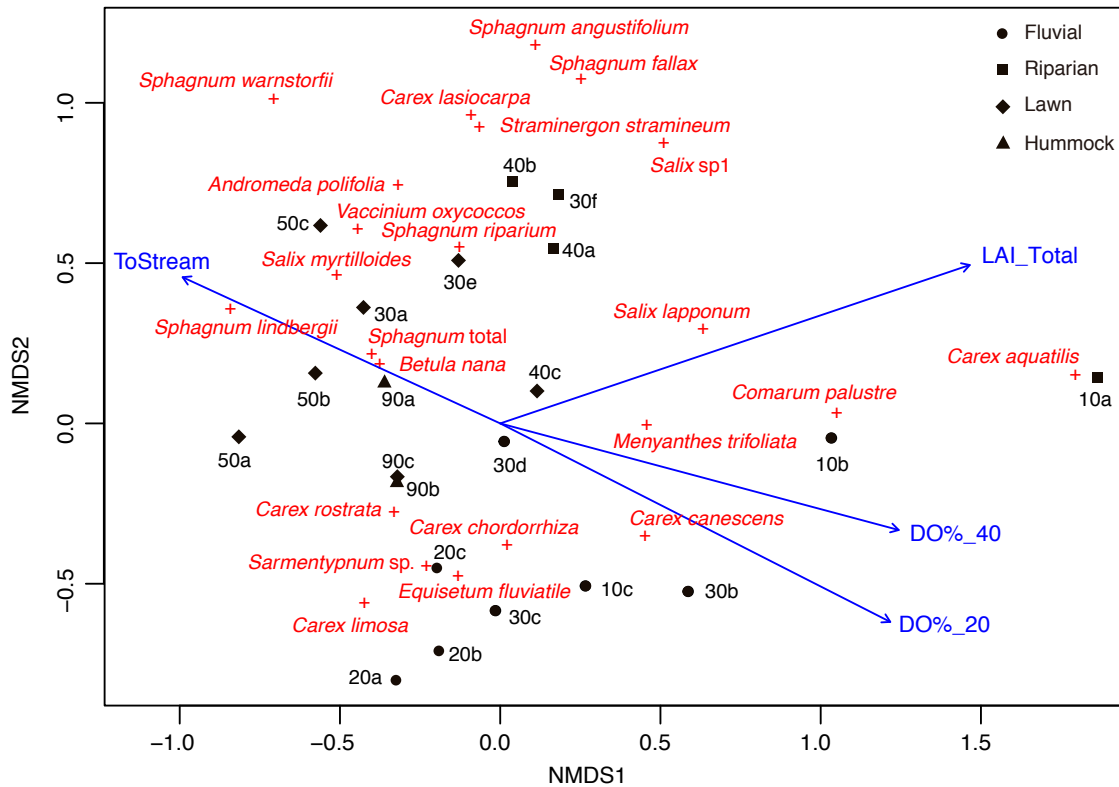


**Figure 3:** Non-metric multidimensional scaling (NMDS; stress 0.15) ordination showing peak season (late July) vegetation structure in the sample plots, including distance to stream (ToStream, $p = 0.042$), peak season (early summer) dissolved oxygen concentration at 20 cm (DO%_20, $p = 0.006$) and 40 cm depths (DO%_40, $p = 0.015$), and peak season (late July) total vascular plant leaf area index (LAI_Total, $p = 0.003$) as fitted environmental variables. Four plant community types that were derived from the regional vegetation data are indicated using different symbols.

## 3.2 Variations in CH₄ fluxes

Measured CH₄ fluxes ranged from 0.16 to 13.78, 0.08 to 23.05, and 0.21 to 26.55 mg m$^{-2}$ h$^{-1}$ in 2017, 2018 and 2019, respectively (Figure 4). In all three years, CH₄ fluxes increased gradually from the early summer, peaking in early August, after which the fluxes decreased. In 2018 and 2019, higher fluxes (> 20 mg m$^{-2}$ h$^{-1}$) were observed in the middle of the growing season compared to 2017 (< 15 mg m$^{-2}$ h$^{-1}$).
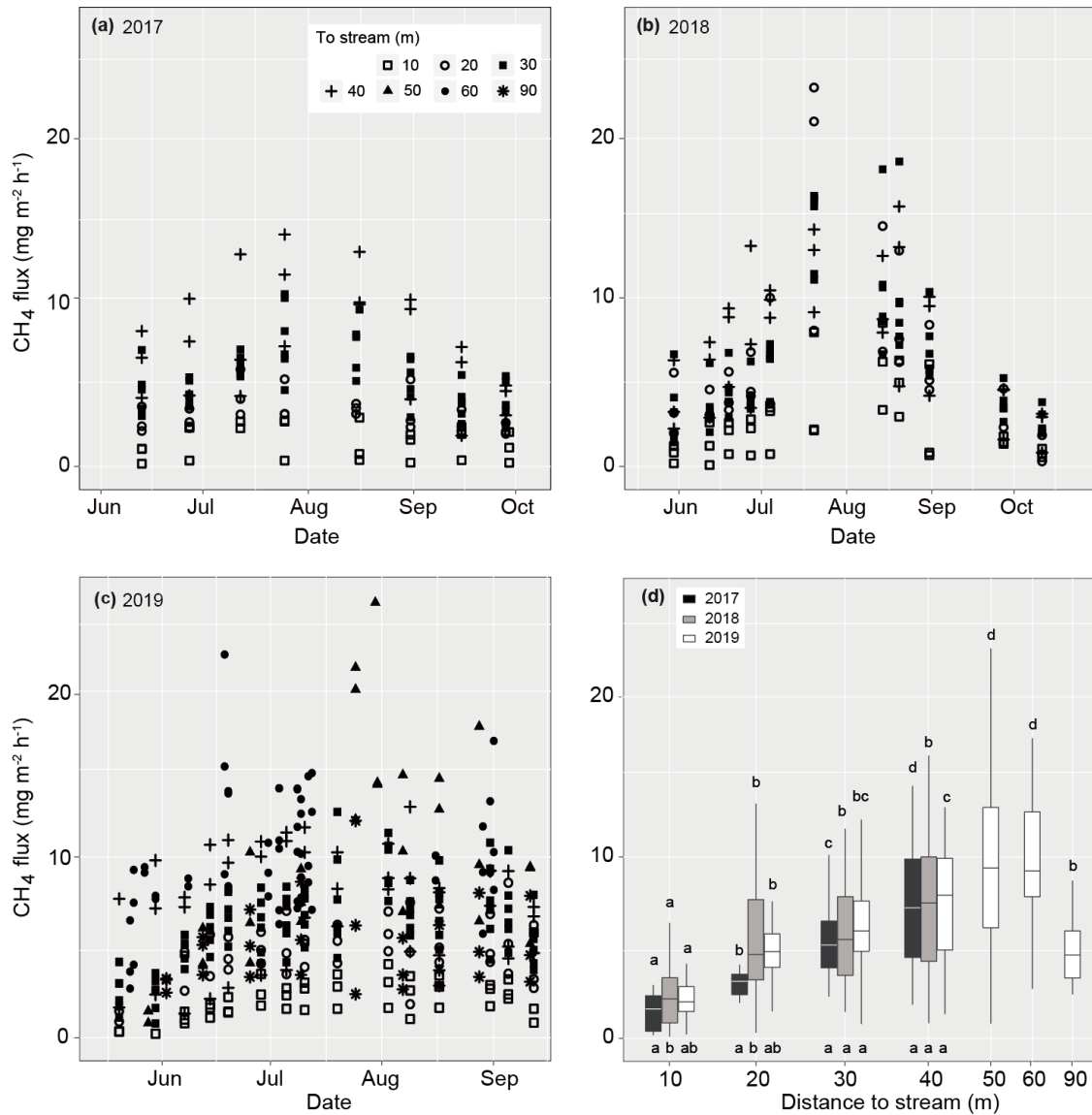
**Figure 4:** Measured methane ($CH_4$) fluxes during the growing season in (a) 2017, (b) 2018, and (c) 2019 at Lompolojänkkä. Distance to the stream of the sample plot clusters are indicated by different symbols. (d) Box plots of $CH_4$ fluxes for each measurement cluster in 2017, 2018 and 2019. The different letters on top of the box plots indicate significant differences ($p < 0.05$) between the clusters for each year, calculated using Tukey's Honest Significant Difference method, and the different letters below the box plots indicate significant differences ($p < 0.05$) between the studied years for each cluster.

Even though there were variations in $CH_4$ fluxes within the sample plot clusters, clear spatial patterns related to their distance to the stream were also evident (Figure 4). In all three years, $CH_4$ fluxes next to the stream (cluster 10) were the lowest. In 2019, when additional sample plots were established (see Materials and methods), fluxes peaked at a 50 m

12

310    distance from the stream. In the previous two years, when sampling only took place to a distance of 40 m from the stream, there was an increasing trend in fluxes with distance. In 2017, $CH_4$ fluxes measured from the various sample plot clusters were significantly different from each other. In 2018, $CH_4$ fluxes from clusters 20–40 were similar, but were significantly higher than the clusters located next to the stream (cluster 10).

Close to the stream, $CH_4$ emissions differed between years; emissions from clusters 10 and 20 were significantly lower in
315    2017 than in 2018, while emissions in 2019 were intermediate and did not differ from the previous two years. At the intermediate distance (clusters 30 and 40), $CH_4$ emissions were at the same level in all three years.

### 3.3 Response of $CH_4$ fluxes to environmental forcing

In the mixed-effect model (three-year dataset), which was constructed to examine spatial variability, $CH_4$ fluxes were controlled by the distance to the stream and by air temperature (fixed predictors), while plant community type was not a
320    significant predictor when distance to the stream was included (Table A3a). There was a quadratic relationship between $CH_4$ fluxes and distance to the stream, with the highest fluxes observed at an intermediate distance (Figure 5a). There was a positive linear correlation between air temperature and $CH_4$ fluxes only at temperatures above a threshold value of 18 °C. Below that threshold, $CH_4$ fluxes remained unaffected (Figure 5). There was a significant interaction between distance to the stream and air temperature ($p = 0.03$), with the greater impact of temperature on $CH_4$ flux observed at plots closer to the
325    stream (Figure 5b).
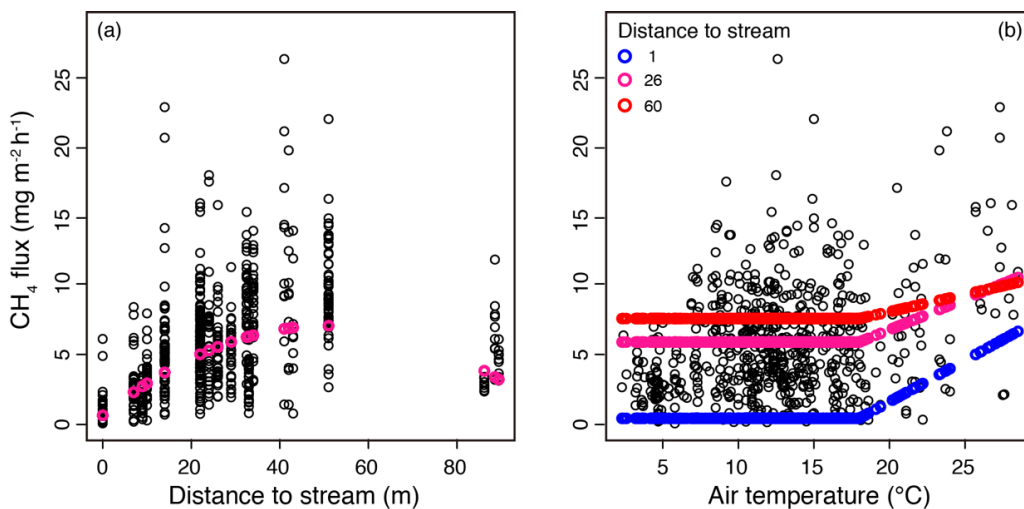


**Figure 5:** Results of mixed-effect model constructed to examine the spatial variation in methane ($CH_4$) fluxes in the valley fen using a three-year dataset. Response curves of $CH_4$ flux to (a) distance to stream, with air temperature kept constant at 18 °C, (b) air temperature,
330    with distance to stream kept constant at 1 m (blue), 26 m (pink) and 60 m (red).

In the second model (2019 dataset), which was constructed to provide a robust mechanistic understanding of $CH_4$ dynamics in the fen, temporal and spatial variation in $CH_4$ flux were found to be best explained by peat temperature at 5 cm (T5), WT, DO concentration at 20 cm below the surface (DO20), graminoid LAI and vascular LAI as fixed predictors (Figure 6, Table A3b). When DO20 was included, the distance to the stream and plant community type were not significant predictors. Of these predictors, DO20 linearly decreased the flux until a threshold value of 40 % was reached, above which it remained constant, while there was a linear relationship between $CH_4$ fluxes and the other predictors (Figure 6). Both T5 and graminoid LAI were observed to linearly increase $CH_4$ fluxes, while fluxes were negatively correlated with WT and vascular LAI (i.e., fluxes were lower at higher water levels and greater vascular LAI values). DO20 interacted with T5 and WT (Figure 6e, f), so that DO20 decreased $CH_4$ flux more steeply at lower T5 and WT values. Also, T5 and WT responses were steeper at low DO20 values. Furthermore, vascular LAI had less impact on $CH_4$ flux at high WT levels.
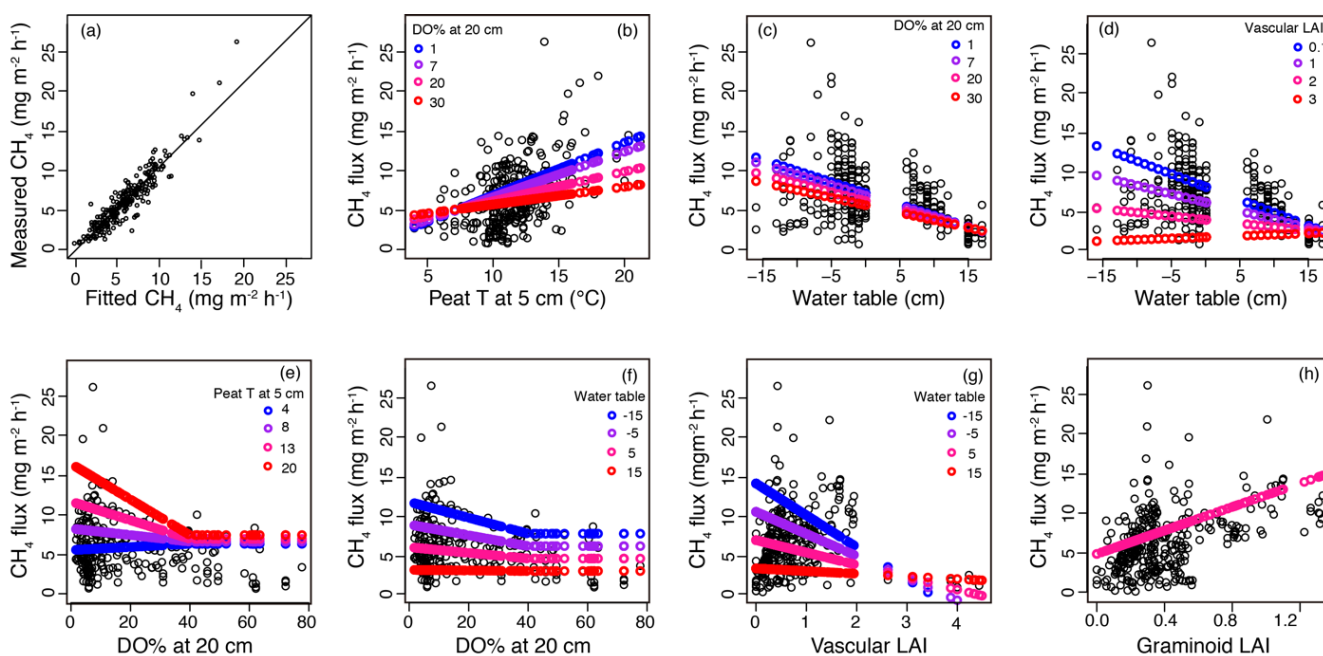


**Figure 6:** Results of the mixed-effect model, which was constructed to provide a robust mechanistic understanding on the controls of methane ($CH_4$) flux in the valley fen using the 2019 data set. (a) Measured $CH_4$ flux values plotted against fitted values of the mixed-effect model. (b-h) Response curves of $CH_4$ flux to (b) peat temperature (T) at 5 cm below the surface, (c, d) water table, (e, f) dissolved oxygen concentration (DO%) at 20 cm below the surface, (g) vascular plant leaf area index (LAI) and (h) graminoid plant LAI with the interactive variable adjusted at four different levels (indicated by four different colours) and the other variables kept constant. When setting variables as constant, the median values of the dataset were chosen, i.e. 11 °C for peat T at 5 cm, -11 (response to DO % at 20 cm) and -1 cm (other responses) for water table, 7 for DO% at 20 cm (when < 40 %), 0.6 for vascular LAI and 0.3 for graminoid LAI.

14

# 4 Discussion

## 4.1 The role of the stream in driving fen vegetation and biomass production

As hypothesised, the spatial heterogeneity in environmental variables in this valley fen site was highly related to the distance from the stream. Peatlands typically have spatially heterogeneous microhabitats due to wide variations in hydrology and nutrient availability (Rydin and Jeglum, 2013), which impact microbial activities and subsequent $CH_4$ emissions (Juottonen et al., 2005; Juottonen et al., 2015; Noyce et al., 2014; Ström et al., 2003). Water table level is one of the most important influences on plant occurrence and growth in peatlands (Rydin and Jeglum, 2013), and in this study, was highest closer to the stream. As a result, hydrophilic species, such as *C. aquatilis*, *S. lapponum*, *C. palustre*, and *M. trifoliata,* were abundant in places close to the stream. Even though we did not measure the chemical composition of the water, the abundance of these species implies a minerogenic supply established by water flow (Wassen et al., 1990).

The observed positive link between early summer oxygen concentrations (a proxy for flowing water) and total LAI further confirmed that flowing water likely delivers more nutrients and better supply plant growth and photosynthesis, and therefore provides more C substrates for microbial activities (Bellisario et al., 1999). In addition, GPP, the key driver of the peatland C cycle (Whiting and Chanton, 1993) and influences peatland vegetation composition and abiotic factors, such as air temperature and water level (Peichl et al., 2018), was consistently higher in plots located nearer the stream. Similarly, dissolved oxygen concentrations that acted as a proxy of the mineral-nutrient rich water were also higher in those plots. It has been shown that increased water supply alone can cause substantial increases in biomass on nutrient-rich soils, while fertilisation/nutrient addition has little effect (Eskelinen and Harrison, 2015). As such, the forbs and mosses that dominate such wet fens might benefit from higher water tables for biomass production (Mäkiranta et al., 2018). In this study, as the stream can bring both water and nutrients to the site at the same time, we are not able to distinguish whether the impact of the stream on the vegetation at our site was caused by the water or by nutrient supply, or both. Nevertheless, our results suggest that flowing water acted as a decisive factor on peatland vegetation composition and biomass production, through the addition of either water or nutrients. Therefore, the stream is likely to play a key role in regulating peatland $CH_4$ emission patterns.

## 4.2 Role of stream-induced microhabitats in driving $CH_4$ emissions

Consistent with our second hypothesis, the overall pattern of $CH_4$ fluxes showed clear spatial variations in relation to the distance from the stream. The impact of the stream was greater than the influence of vegetation community types, which represent general microform conditions and have been commonly reported to regulate $CH_4$ emissions (e.g., Riutta et al., 2007). Specifically, as expected in the third hypothesis, factors such as peat temperature at 5 cm depth (T5), WT, DO20 and LAI, which were to some extent shaped by the stream, were all significant factors in driving $CH_4$ emissions at this site.

Our data suggest that $CH_4$ emissions increased with higher T5 values, similarly to many previous studies (e.g., Korrensalo et al., 2018; Rinne et al., 2018). Rising temperature is known to increase the activity of $CH_4$ producing microbes, and also enhance $CH_4$ transport through aerenchymous plants (Dunfield et al., 1993; Grosse, 1996; Kolton et al., 2019). Moreover,

385    the temperature sensitivity in our study site was stronger closer to the stream, which is possibly due to a higher dissolution rate in cold water. The pattern implies that in the fertile conditions next to the stream, higher oxygen concentrations in the cool water limits emissions by supressing $CH_4$ production or by enhancing oxidation, and that warming of the water removes this limitation. In support of this finding, higher DO20 values were found to decrease temperature sensitivity. Similar to the $CH_4$ response to T5, higher DO20 values also reduced the impact of WT position on $CH_4$ emissions. Both responses

390    highlight the importance of oxidation when considering how $CH_4$ emissions respond to environmental changes (Song et al., 2020). The patterns might also indicate higher $CH_4$ production under warmer conditions within the catchment and, consequently, on higher $CH_4$ concentrations in the flowing water (Juutinen et al., 2013). However, in this study we were not able to determine the origin of the emitted $CH_4$.

    In our sampling campaign, WT levels were observed both above and below the soil surface, and $CH_4$ emissions were found

395    to generally decrease with rising WT levels. This decrease is in contradiction with many other studies that mainly cover sites with WT levels below the soil surface (Bubier et al., 2005; Pelletier et al., 2007; Turetsky et al., 2008). However, low emissions were also observed in the drier parts of the fen, which is in agreement with previous studies, in addition to very low emissions observed close to the stream. The lower emissions and a generally unimodal response to WT level were overridden in the whole dataset by the much stronger pattern captured close to the stream. Two plausible explanations for the

400    observed WT–$CH_4$ emission pattern are, 1) the potential $CH_4$ production zone is smaller and the potential $CH_4$ oxidation zone is greater in drier conditions (Lai, 2009), and 2) in wet conditions, where there is moving water, lower $CH_4$ emissions can be attributed to enhanced $CH_4$ oxidation in the oxygen-rich water column, and a lower $CH_4$ production rate due to the presence of oxygen (Bubier, 1995). Also, lower peat temperatures due to the higher water table and flowing water likely contribute to a lower $CH_4$ production rate.

405    In our study, vascular LAI was found to have a negative linear correlation with $CH_4$ emissions. Plots nearest the stream had the highest vascular LAI values but the lowest $CH_4$ fluxes, i.e. the impact of the stream was again predominant over the impact of LAI. Studies have shown that shrubs can hinder $CH_4$ production because of their poor-quality substrate for methanogenesis (Riutta et al., 2020, Yavitt et al., 2019), although the cover of shrubs at our study site was very small. Therefore, low $CH_4$ emissions at high vascular LAI values is likely due to *in situ* lower peat temperature and the higher

410    oxygen concentrations caused by the moving water. As aerenchymous LAI showed a very similar pattern to vascular LAI, it was not included in the mechanistic model. Instead, graminoid LAI, which was not impacted by the stream, showed a positive link with $CH_4$ emissions, which is in line with several previous studies (e.g. Bhullar et al., 2013ab). The exceptionally high $CH_4$ fluxes measured at cluster 50 where the graminoid LAI was low is potentially linked to one aerenchymous species growing in the cluster, i.e. *Eriophorum vaginatum*, which can enhance $CH_4$ release and increase C

415    substrate input to methanogens (Greenup et al., 2000).

    In general, $CH_4$ emissions in stream-dominated fens are likely to show a quadratic response pattern in regard to their distance to the stream, with low emissions occurring at both the closest and farthest locations from the stream, mainly due to high oxygen concentrations and water depletion, respectively. The highest $CH_4$ emissions were found in places at intermediate

distances to the stream, which benefit from both sufficient water and nutrient supply but have inherently low soil oxygen concentrations. However, we acknowledge the challenge of defining the stream at our site due to the seasonal variation in catchment hydrological conditions. Hence, this study only demonstrates the stream-CH$_4$ emission pattern, rather than providing quantitative information for projections.

### 4.3 Future peatland CH$_4$ emission trajectories under climate change

Projection of global peatland CH$_4$ emissions under different climate change scenarios is a major challenge due to the reported variabilities in emissions, and also because of the interactions between the various environmental predictors (Strack and Waddington, 2007; Strack et al., 2004; Weltzin et al., 2000; Zhang et al., 2002). Our study further highlights that the impacts of climate change on CH$_4$ emissions in flow-through peatland systems are even more complicated due to the additional effects of the flowing water, which poses a challenge for accurate predictions of the global CH$_4$ budget. Nevertheless, despite the complexity, clear patterns emerged that are informative in placing current peatland habitat-based CH$_4$ emission measurements into a broader context, and supplement the current understanding of peatland CH$_4$ emissions (Figure 7).
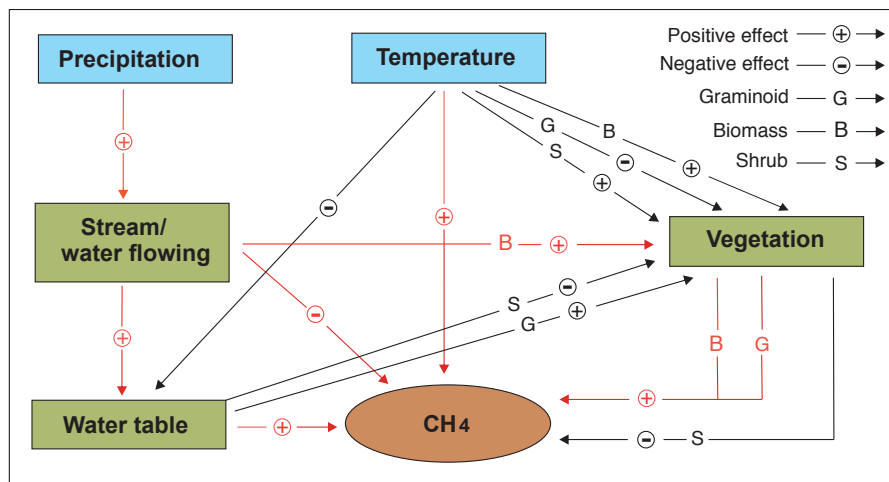


**Figure 7:** Schematic illustration showing the potential independent and interactive impacts of precipitation, temperature, vegetation and hydrology on methane (CH$_4$) fluxes in northern peatlands. Arrows in red and black are derived from this study and previous studies, respectively (e.g., Mäkiranta et al., 2018; Roulet et al., 1992; Yavitt et al., 2019).

The majority of peatlands are located in northern high latitudes where the climate is currently experiencing a greater rate of change than in other regions (Collins et al., 2013). Climate warming is expected to promote microbial activity, and therefore faster C cycling. However, warming in tandem with drying has been shown to decrease the methanogenic archaea populations (Peltoniemi et al., 2015). In our study, vegetation composition, as such, was not a significant controller of CH$_4$

17

emissions, although biomass production (GPP and LAI), influenced by the stream, was a very important controller as it likely provides substrates for methanogens. However, this is in contradiction with the suggestion that vegetation mainly influences $CH_4$ emissions at minerotrophic sites by facilitating transportation, while at ombrotrophic sites it is through

445  substrate-based interactions regulated by plant photosynthetic activity (Oquist and Svensson, 2002). Climate warming and/or peat surface drying can alter vegetation composition and affect the contribution of the biomass that is produced. For example, shrubs can benefit from these environmental changes, while forbs and mosses may suffer (Kokkonen et al. 2019, Mäkiranta et al., 2018, Strack et al. 2006). Even though such hydroclimatic impacts on vegetation might be modified by nitrogen availability (Luan et al., 2019), high latitudes generally experience little nitrogen deposition (Du et al., 2020). The abundance

450  and functional types of the plants, especially graminoid plants, regulate $CH_4$ fluxes, but such impacts might be overruled if the water table level drops substantially (Riutta et al., 2020). In addition, there is some evidence of microtopographic differences in peatland nutrient dynamics in response to drying (Macrae et al., 2013), whereas flowing water will benefit the nutrient supply at a specific site. Furthermore, the expansion of shrubs, in response to drying, might potentially decrease peat temperatures due to increased shading and the evaporative cooling effect (Strakova et al., 2012), and thereby reduce $CH_4$

455  emissions.

Flowing water also tends to keep the peat temperature lower, even though fens with moving water warm up earlier than other peatlands in the spring and early summer (Rydin and Jeglum, 2013). In contrast to temperature predictions, predicting precipitation remains more uncertain, although in general, it is expected to increase in several regions (Collins et al., 2013). Although peatland hydrological processes are not directly impacted by precipitation due to, for example, evapotranspiration

460  and runoff, it has been shown that precipitation can decrease $CO_2$ uptake and GPP due to cloudiness and associated reduced light availability (Nijp et al., 2015), thus influencing $CH_4$ emissions. Precipitation can also cause more dynamics of water and decrease $CH_4$ emissions by providing more oxygen for $CH_4$ oxidation (Mitchell and Branfireun 2005, Radu and Duval 2018), which can be further accelerated under a warmer and drier peat surface scenario.

465  **5 Conclusions**

Our data from a flow-through valley fen demonstrates that hydrology in northern fen systems has a dual role in controlling $CH_4$ emissions, depending on the presence or absence of a stream. Flowing water not only enhances nutrient transportation and oxygen availability, but also decreases peat temperature, all of which are significant direct or indirect controllers of $CH_4$ emissions. At places close to the stream there were higher water levels, lower peat temperatures, and greater oxygen

470  concentrations; these supported the highest total leaf area and gross primary production rates but resulted in the lowest $CH_4$ emissions. Further from the stream, the conditions were drier and $CH_4$ emissions were also low. $CH_4$ emissions were highest in the intermediate distance from the stream where oxygen concentration in the surface peat was low but gross primary production was still high. Our results show how a stream controls $CH_4$ emissions in a flow-through fen, which is a common peatland ecosystem type from the arctic to the temperate zones. Therefore, future projections of the global $CH_4$ budget need

475  to take into account flowing water features in fen systems.

**Appendices**
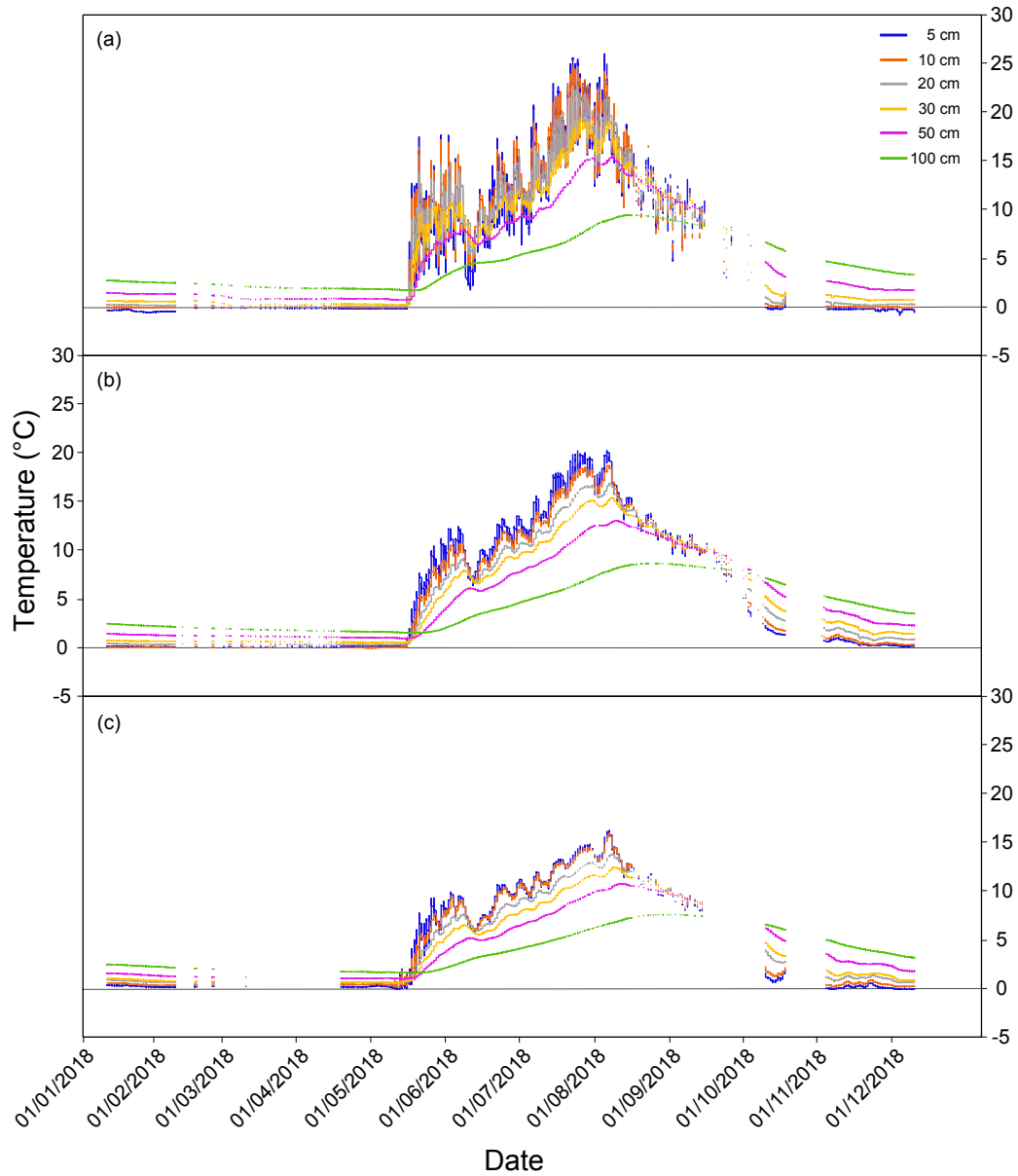


**Figure A1:** Continuous peat temperature (at 5, 10, 20, 30, 50 and 100 cm depth below the surface) in 2018 at Lompolojänkka at measuring points, (a) far from the stream, (b) intermediate distance to the stream, and (c) in the stream. Detailed description of the locations of the sample points can be found in Figure 1.
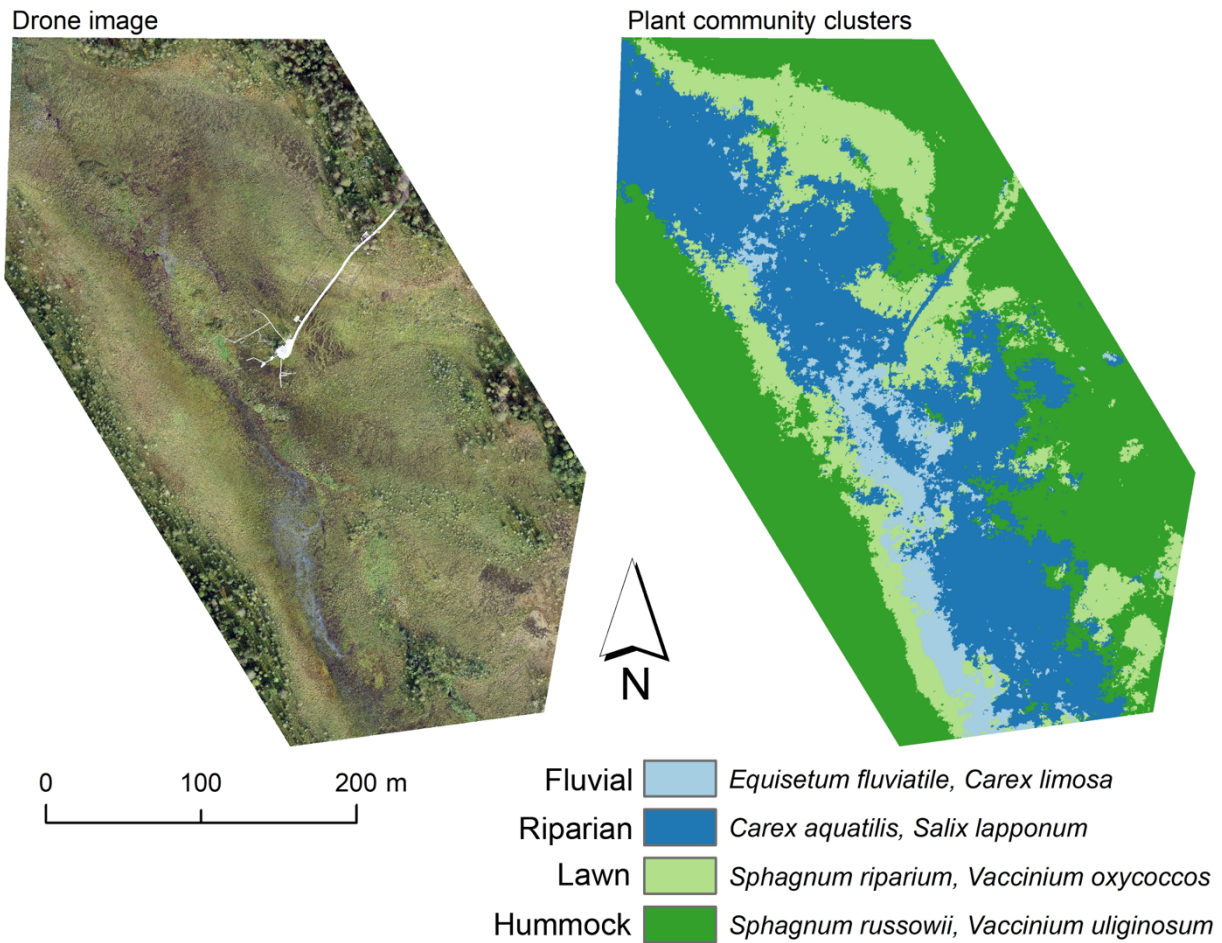
**Figure A2:** Drone image and a map of plant community clusters over the study area. The cluster map was produced with the multi-source remote sensing data listed in Räsänen et al. (2020). We calculated remote sensing features for the vegetation plots and vegetation patches delineated from the drone image with mean-shift segmentation in Orfeo ToolBox (Grizonnet et al. 2017). We trained a random forest classification (Breiman 2001) with the vegetation plot data and predicted the classification for the vegetation patches. Classification accuracy (random forest out-of-bag estimate) was 61 %.
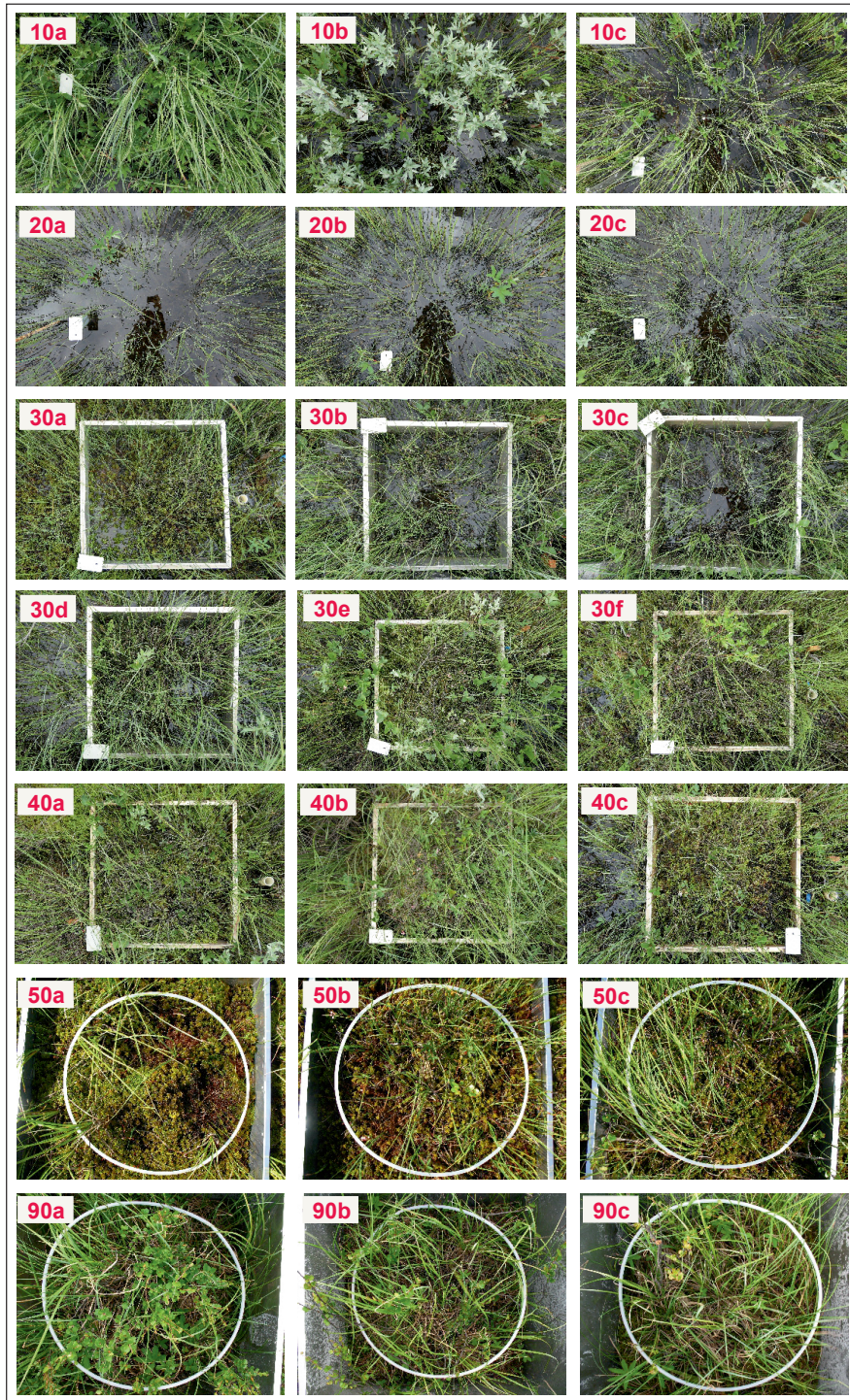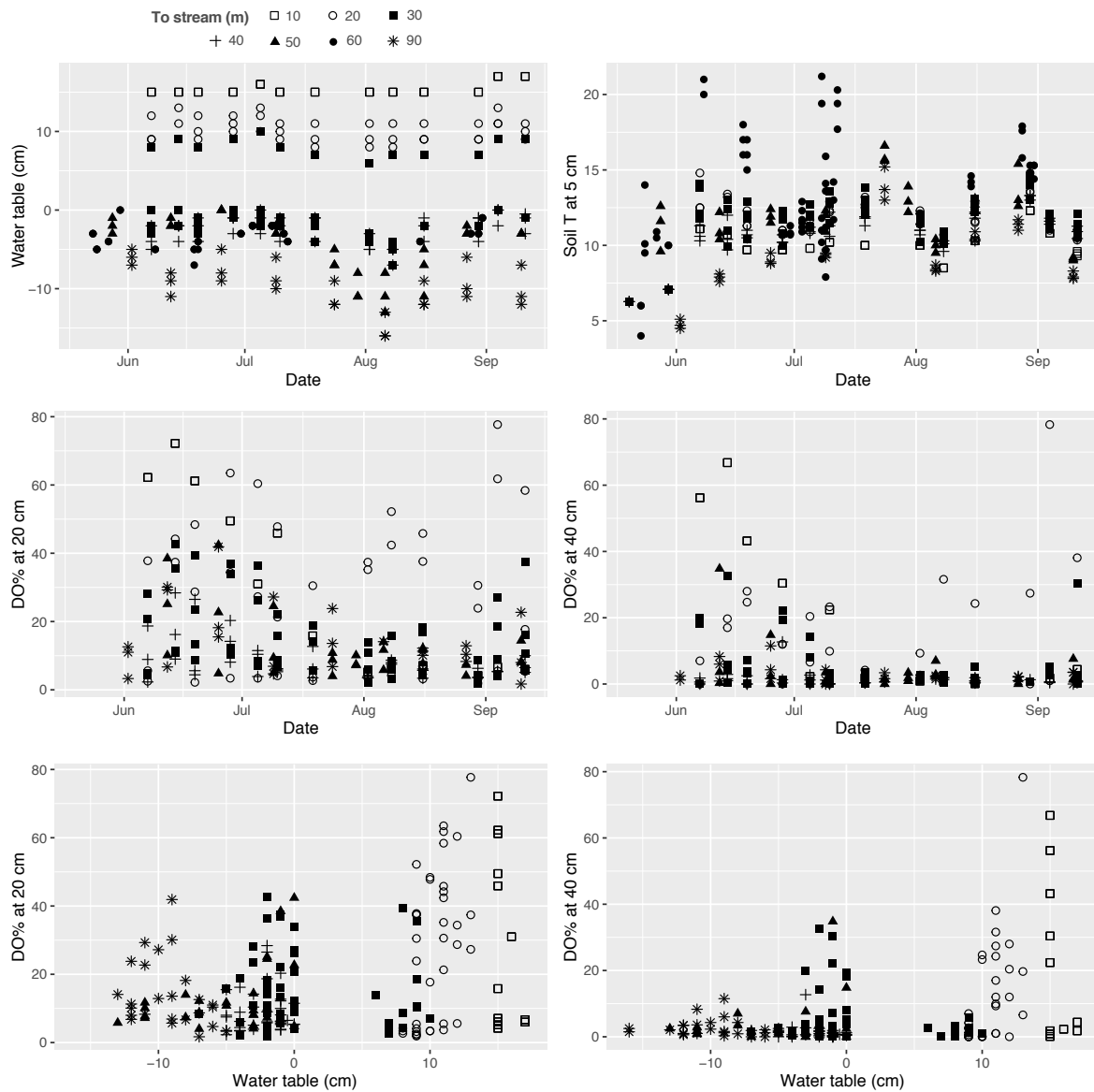
490

**Figure A3:** Photos of the methane ($CH_4$) flux sample plots at Lompolojänkkä taken on 1 July 2019 (clusters 10 to 40) and 28 June 2019 (clusters 50 and 90). Photos for cluster 60 were not taken.

495

**Figure A4:** Upper two panels: temporal variations in water table, soil temperature (T) at 5 cm below the peat surface, and dissolved oxygen concentration (DO%) at 20 cm and 40 cm below the surface during the 2019 growing season at each methane (CH$_4$) flux sample plot. Lower panel: DO% at 20 and 40 cm plotted against water table. Plots in the same cluster are labeled using the same symbol.
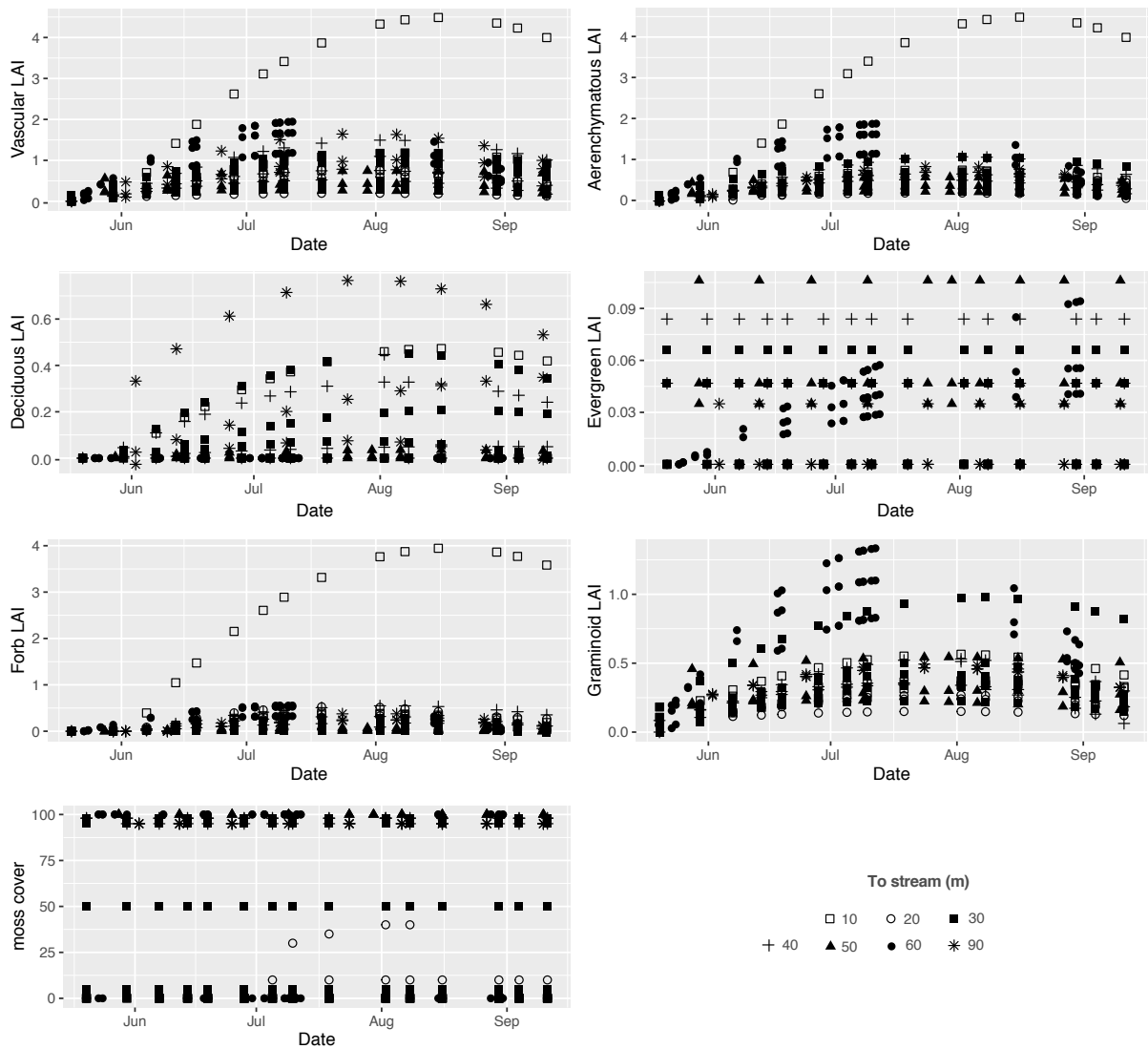
500

**Figure A5:** Temporal development of leaf area index (LAI) for total vascular, aerenchymous, deciduous, evergreen, forb, and graminoid plants, and moss cover (%) in each methane ($CH_4$) flux sample plot. Plots in the same cluster are labeled using the same symbol.

505

23
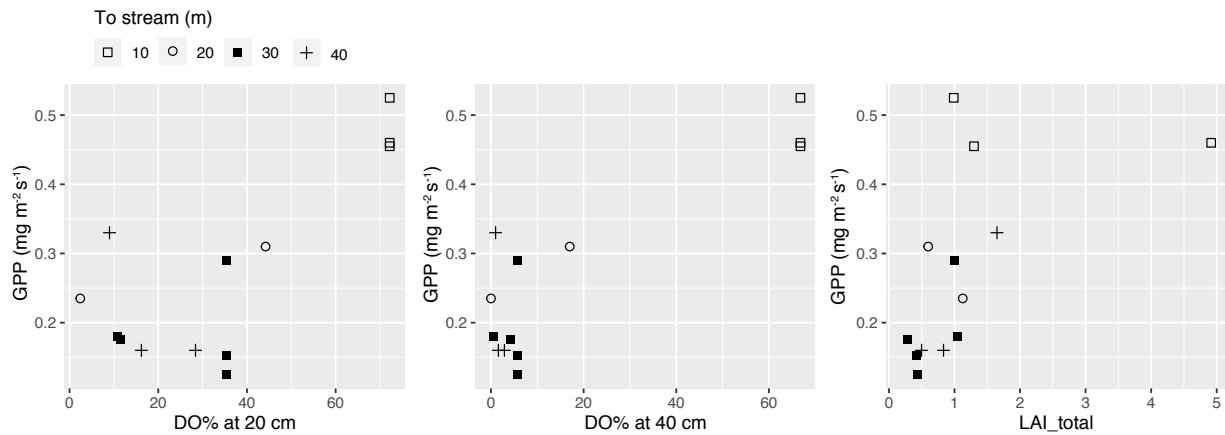
**Figure A6:** Gross primary production (GPP) at a photosynthetic photon flux density level of 800 µmol m$^{-2}$ s$^{-1}$ in the methane (CH$_4$) flux sample plots in clusters 10–40 plotted against peak season (early summer) dissolved oxygen concentration (DO%) at 20 and 40 cm below the surface, and peak season (late July) total vascular leaf area index (LAI_total). Plots in the same cluster are labeled using the same symbol.



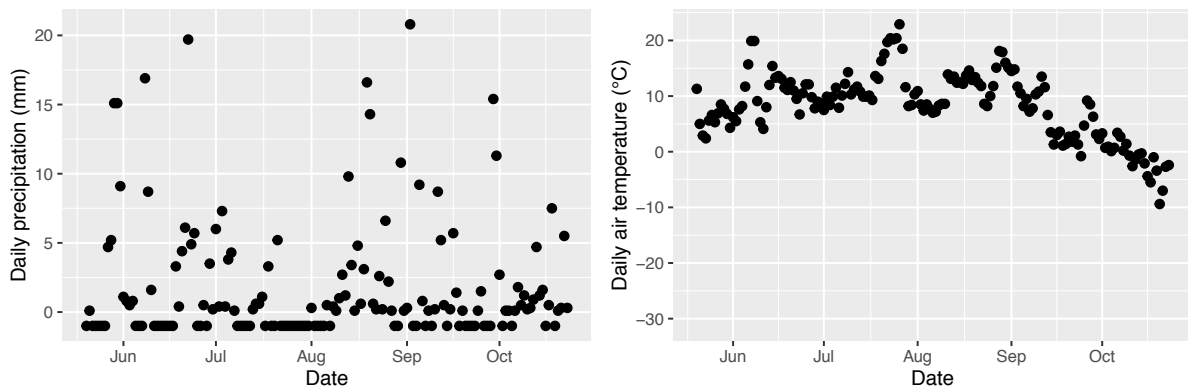**Figure A7:** Daily precipitation and air temperature at Lompolojänkkä during summer 2019. Data were originated from the nearest weather stations; Lompolonvuoma (for temperature) and Kenttärova (for precipitation).

24

530 **Table A1:** Equations for calculating leaf area index (LAI) for four plant functional types (PFTs) based on %-cover (c) and height (h; cm) data.

| PFT | Equation | RMSE | Adj.$R^2$ |
|---|---|---|---|
| evergreen shrub | LAI = 0.023066 + 0.011866*c | 0.1413066 | 0.7488 |
| deciduous shrub | LAI = -0.034458 + 0.020706*c | 0.3275706 | 0.7261 |
| forb | LAI = -2.193e-02 + 1.360e-03*c*h | 0.188271 | 0.8877 |
| graminoid | LAI = 0.045542 + 0.024965*c | 0.1697018 | 0.7346 |

535 **Table A2:** Indicator plant species of plant community clusters of the methane ($CH_4$) flux sample plots derived from non-metric multidimensional scaling (NMDS) analysis.

| Species | Cluster | Indicator_value | Species | Cluster | Indicator_value | Species | Cluster | Indicator_value |
|---|---|---|---|---|---|---|---|---|
| *Equisetum fluviatile* | 1 | 0.505 | *Menyanthes trifoliata* | 2 | 0.208 | *Empetrum nigrum* | 4 | 0.254 |
| *Carex limosa* | 1 | 0.355 | *Sphagnum riparium* | 3 | 0.361 | *Sphagnum fallax* | 4 | 0.189 |
| *Carex canescens* | 1 | 0.116 | *Vaccinium oxycoccos* | 3 | 0.284 | *Aulacomnium palustre* | 4 | 0.188 |
| *Maksasammal sp.* | 1 | 0.088 | *Carex livida* | 3 | 0.194 | *Carex pauciflora* | 4 | 0.143 |
| *Sarmentypnum sarmentosum* | 1 | 0.080 | *Sphagnum lindbergii* | 3 | 0.146 | *Eriophorum vaginatum* | 4 | 0.086 |
| *Carex aquatilis* | 2 | 0.429 | *Sphagnum russowii* | 4 | 0.538 | *Picea abies* | 4 | 0.076 |
| *Salix lapponum* | 2 | 0.380 | *Vaccinium uliginosum* | 4 | 0.536 | *Vaccinium vitis-idaea* | 4 | 0.076 |
| *Salix phylicifolia* | 2 | 0.278 | *Betula nana* | 4 | 0.441 | *Dicranum sp.* | 4 | 0.073 |
| *Mnium sp* | 2 | 0.273 | *Sphagnum total* | 4 | 0.402 | *Sphagnum compactum* | 4 | 0.061 |
| *Comarum palustre* | 2 | 0.250 | *Rubus chamaemorus* | 4 | 0.394 | *Equisetum sylvaticum* | 4 | 0.061 |
| *Sphagnum teres* | 2 | 0.234 | *Sphagnum fuscum* | 4 | 0.275 | | | |

**Table A3:** Parameter estimates of the linear mixed-effect models describing the response of methane ($CH_4$) fluxes to environmental variables in the (a) 2017-2019, and (b) 2019 datasets. Tostream: the distance from the plot to the stream; Tair.18: air temperature greater than the threshold value 18 °C; T5: peat temperature at 5 cm depth below the surface; DO20.40: dissolved oxygen concentration at 20 cm depth below the surface lower than the threshold value 40%; WT: water level relative to the moss surface; G_LAI: graminoid LAI; V_LAI: vascular LAI.

(a) marginal $R^2 = 0.32$, conditional $R^2 = 0.74$

| | Coeff. | SE | DF | $t$-value | $P$-value |
|---|---|---|---|---|---|
| **Fixed part** | | | | | |
| Intercept | 0.181 | 0.591 | 348 | 0.306 | 0.760 |
| Tostream | 0.298 | 0.021 | 243 | 14.406 | 0.000 |
| Tair.18 | 0.597 | 0.097 | 348 | 6.188 | 0.000 |
| I(Tostream^2) | -0.003 | 0.000 | 243 | -12.193 | 0.000 |
| Tostream:Tair.18 | -0.006 | 0.003 | 348 | -2.167 | 0.031 |
| **Random part** | | | | | |
| SD (measured year) | 0.000 | | | | |
| SD (measured month) | 1.821 | | | | |
| SD (plot) | 1.702 | | | | |
| Residual SD | 1.967 | | | | |

(b) marginal $R^2 = 0.42$, conditional $R^2 = 0.87$

| | Coeff. | SE | DF | $t$-value | $P$-value |
|---|---|---|---|---|---|
| **Fixed part** | | | | | |
| Intercept | -1.158 | 1.938 | 100 | -0.598 | 0.551 |
| T5 | 0.690 | 0.160 | 90 | 4.320 | <0.001 |
| DO20.40 | 0.118 | 0.075 | 220 | 1.576 | 0.116 |
| WT | -0.364 | 0.066 | 104 | -5.513 | <0.001 |
| G_LAI | 7.514 | 2.239 | 138 | 3.356 | 0.001 |
| V_LAI | -2.205 | 0.725 | 200 | -3.041 | 0.003 |
| T5:DO20.40 | -0.015 | 0.006 | 217 | -2.430 | 0.016 |
| DO20.40:WT | 0.003 | 0.001 | 233 | 2.272 | 0.024 |
| WT:V_LAI | 0.125 | 0.045 | 207 | 2.771 | 0.006 |
| **Random part** | | | | | |
| | Variance | SD | | | |
| measurement day | 1.636 | 1.279 | | | |
| plot | 5.459 | 2.336 | | | |
| Residual | 1.976 | 1.406 | | | |

## Data availability

The data used in this study will be made available on the Figshare repository after the article is accepted for publication.

## Author contribution

## Competing interests

The authors declare that they have no conflict of interest.

## Acknowledgements

## References

Abdalla, M., Hastings, A., Truu, J., Espenberg, M., Mander, U., and Smith, P.: Emissions of methane from northern peatlands: a review of management impacts and implications for future management options. *Ecol Evol, 6*(19), 7080-7102. doi:10.1002/ece3.2469, 2016.

Aerts, R., Verhoeven, J. T. A., and Whigham, D. F.: Plant-mediated controls on nutrient cycling in temperate fens and bogs. *Ecology, 80*(7), 2170-2181. doi:10.1890/0012-9658(1999)080 [2170:Pmconc]2.0.Co;2, 1999.

Alm, J., Shurpali, N. J., Tuittila, E. S., Laurila, T., Maljanen, M., Saarnio, S., and Minkkinen, K.: Methods for determining emission factors for the use of peat and peatlands - flux measurements and modelling. *Boreal Environ Res, 12*(2), 85-100, 2007.

Andersen, R., Poulin, M., Borcard, D., Laiho, R., Laine, J., Vasander, H., and Tuittila, E. T.: Environmental control and spatial structures in peatland vegetation. *J Veg Sci, 22*(5), 878-890. doi:10.1111/j.1654-1103.2011.01295.x, 2011.

Aurela, M., Lohila, A., Tuovinen, J. P., Hatakka, J., Riutta, T., and Laurila, T.: Carbon dioxide exchange on a northern boreal fen. *Boreal Environ Res, 14*(4), 699-710, 2009.

Bellisario, L. M., Bubier, J. L., Moore, T. R., and Chanton, J. P.: Controls on $CH_4$ emissions from a northern peatland. *Global Biogeochem Cy, 13*(1), 81-91. doi:10.1029/1998gb900021, 1999.

Bhullar, G. S., Edwards, P. J., and Venterink, H. O.: Variation in the plant-mediated methane transport and its importance for methane emission from intact wetland peat mesocosms. *J Plant Ecol, 6*(4), 298-304. doi:10.1093/jpe/rts045, 2013a.

Bhullar, G. S., Iravani, M., Edwards, P. J., and Venterink, H. O.: Methane transport and emissions from soil as affected by water table and vascular plants. *Bmc Ecol*, 13. doi:10. 1186/1472-6785-13-32, 2013b.

Bjorkman, A. D., Myers-Smith, I. H., Elmendorf, S. C., Normand, S., Ruger, N., Beck, P. S. A., Blach-Overgaard, A., Blok, D., Cornelissen, J. H. C., Forbes, B. C., Georges, D., Goetz, S. J., Guay, K. C., Henry, G. H. R., HilleRisLambers, J., Hollister, R. D., Karger, D. N., Kattge, J., Manning, P., Prevey, J. S., Rixen, C., Schaepman-Strub, G., Thomas, H. J. D., Vellend, M., Wilmking, M., Wipf, S., Carbognani, M., Hermanutz, L., Levesque, E., Molau, U., Petraglia, A., Soudzilovskaia, N. A., Spasojevic, M. J., Tomaselli, M., Vowles, T., Alatalo, J. M., Alexander, H. D., Anadon-Rosell, A., Angers-Blondin, S., te Beest, M., Berner, L., Bjork, R. G., Buchwal, A., Buras, A., Christie, K., Cooper,

E. J., Dullinger, S., Elberling, B., Eskelinen, A., Frei, E. R., Grau, O., Grogan, P., Hallinger, M., Harper, K. A., Heijmans, M. M. P. D., Hudson, J., Hulber, K., Iturrate-Garcia, M., Iversen, C. M., Jaroszynska, F., Johnstone, J. F., Jorgensen, R. H., Kaarlejarvi, E., Klady, R., Kuleza, S., Kulonen, A., Lamarque, L. J., Lantz, T., Little, C. J., Speed, J. D. M., Michelsen, A., Milbau, A., Nabe-Nielsen, J., Nielsen, S. S., Ninot, J. M., Oberbauer, S. F., Olofsson, J., Onipchenko, V. G., Rumpf, S. B., Semenchuk, P., Shetti, R., Collier, L. S., Street, L. E., Suding, K. N., Tape, K. D., Trant, A., Treier, U. A., Tremblay, J. P., Tremblay, M., Venn, S., Weijers, S., Zamin, T., Boulanger-Lapointe, N., Gould, W. A., Hik, D. S., Hofgaard, A., Jonsdottir, I. S., Jorgenson, J., Klein, J., Magnusson, B., Tweedie, C., Wookey, P. A., Bahn, M., Blonder, B., van Bodegom, P. M., Bond-Lamberty, B., Campetella, G., Cerabolini, B. E. L., Chapin, F. S., Cornwell, W. K., Craine, J., Dainese, M., de Vries, F. T., Diaz, S., Enquist, B. J., Green, W., Milla, R., Niinemets, U., Onoda, Y., Ordonez, J. C., Ozinga, W. A., Penuelas, J., Poorter, H., Poschlod, P., Reich, P. B., Sande, B., Schamp, B., Sheremetev, S., Weiher, E.: Plant functional trait change across a warming tundra biome. *Nature, 562*(7725), 57-62. doi:10.1038/s41586-018-0563-7, 2018.

Bousquet, P., Ringeval, B., Pison, I., Dlugokencky, E. J., Brunke, E. G., Carouge, C., Chevallier, F., Fortems-Cheiney, A., Frankenbery, C., Hauglustaine, D.A., Krummel, P.B., Langenfelds, R.L., Ramonet, M., Schmidt, M., Steele, L.P., Szopa, S., Yver, C., Viovy, N., and Ciais, P.: Source attribution of the changes in atmospheric methane for 2006–2008. *Atmos Chem Phys, 11*(8), 3689-3700. doi:10.5194/acp-11-3689-2011, 2011.

Breiman, L.: Random Forests. Machine Learning, 45, 5-32, 2001

Bubier, J., Moore, T., Savage, K., and Crill, P.: A comparison of methane flux in a boreal landscape between a dry and a wet year. *Global Biogeochem Cy, 19*(1). doi:10. 1029/2004gb002351, 2005.

Bubier, J. L.: The relationship of vegetation to methane emission and hydrochemical gradients in northern peatlands. *J Ecol, 83*(3), 403-420. doi:10.2307/2261594, 1995.

Ciais, P., Sabine, C., Bala, G., Bopp, L., Brovkin, V., Canadell, J., Chhabra, A., DeFries, R., Galloway, J., Heimann, M., Jones, C., Le Quere, C., Myneni, R.B., Piao, S., and Thornton, P.: Carbon and other biogeochemical cycles. *Climate Change 2013: The Physical Science Basis*, 465-570, 2014.

Collins, M., R. Knutti, J. Arblaster, J.-L. Dufresne, T. Fichefet, P. F., X. Gao, Gutowski, W.J., Johns, T., Krinner, G., Shongwe, M., Tebaldi, C., Weaver, A.J., Wehner, M.: Long-term Climate Change: Projections, Commitments and Irreversibility. In: Climate Change 2013: The Physical Science Basis. Contribution of Working Group I to the Fifth Assessment Report of the Intergovernmental Panel on Climate Change [Stocker, T.F., D. Qin, G.-K. Plattner, M. Tignor, S.K. Allen, J. Boschung, A. Nauels, Y. Xia, V. Bex and P.M. Midgley (eds.)]. Cambridge University Press, Cambridge, United Kingdom and New York, NY, USA. 2013.

Du, E. Z., Terrer, C., Pellegrini, A. F. A., Ahlstrom, A., van Lissa, C. J., Zhao, X., Xia, N., Wu, X., and Jackson, R. B.: Global patterns of terrestrial nitrogen and phosphorus limitation. *Nat Geosci,* 13, 221-226. doi:10.1038/s41561-019-0530-4, 2020.

Dunfield, P., Knowles, R., Dumont, R., and Moore, T. R.: Methane production and consumption in temperate and sub-arctic peat soils - Response to temperature and pH. *Soil Biol Biochem, 25*(3), 321-326. doi:10.1016/0038-0717(93)90130-4, 1993.

Eskelinen, A., and Harrison, S. P.: Resource colimitation governs plant community responses to altered precipitation. *P Nati Acad Sci USA, 112*(42), 13009-13014. doi:10.1073/pnas.1508170112, 2015.

Euskirchen, E.S., Kane, E.S., and Turetsky, M.R.: When the source of flooding matters: divergent responses in carbon fluxes in an alaskan rich fen to two types of inundation. Ecosystems, doi:10.1007/s10021-019-00460-z, 2019.

Greenup, A. L., Bradford, M. A., McNamara, N. P., Ineson, P., and Lee, J. A.: The role of *Eriophorum vaginatum* in $CH_4$ flux from an ombrotrophic peatland. *Plant Soil, 227*(1-2), 265-272. doi: 10.1023/A:1026573727311, 2000.

Grizonnet, M., Michel, J., Poughon, V., Inglada, J., Savinaud, M., and Cresson, R.: Orfeo ToolBox: open source processing of remote sensing images. Open Geospatial Data, Software and Standards, 2(1). doi:10.1186/s40965-017-0031-6, 2017.

Grosse, W.: The mechanism of thermal transpiration (equals thermal osmosis). *Aquat Bot, 54*(2-3), 101-110. doi:10.1016/0304-3770(96)01038-8, 1996.

Hajek, T., Tuittila, E. S., Ilomets, M., and Laiho, R.: Light responses of mire mosses - a key to survival after water-level drawdown? *Oikos, 118*(2), 240-250. doi:10.1111/j.1600-0706.2008.16528.x, 2009.

Helbig, M., Waddington, J. M., Alekseychik, P., D.Amiro, B., Aurela, M., Barr, A. G., Black, T. A., Blanken, P. D., Carey, S. K., Chen, J. Q., Chi, J. S., Desai, A. R., Dunn, A., Euskirchen, E. S., Flanagan, L. B., Forbrich, I., Friborg, T., Grelle, A., Harder, S., Heliasz, M., Humphreys, E. R., Ikawa, H., Isabelle, P. E., Iwata, H., Jassal, R., Korkiakoski,

635 M., Kurbatova, J., Kutzbach, L., Lindroth, A., Lofvenius, M. O., Lohila, A., Mammarella, I., Marsh, P., Maximov, T., Melton, J. R., Moore, P. A., Nadeau, D. F., Nicholls, E. M., Nilsson, M. B., Ohta, T., Peichl, M., Petrone, R. M., Petrov, R., Prokushkin, A., Quinton, W. L., Reed, D. E., Roulet, N. T., Runkle, B. R. K., Sonnentag, O., Strachan, I. B., Taillardat, P., Tuittila, E. S., Tuovinen, J. P., Turner, J., Ueyama, M., Varlagin, A., Wilmking, M., Wofsy, S. C. and Zyrianov, V.: Increasing contribution of peatlands to boreal evapotranspiration in a warming climate. Nat Clim Cha[...] doi:10.1038/s41558-020-0763-7, 2020.

640 Ingram, H. A. P.: *Hydrology. Mires: Swamp, bog, fen, and moor.* Amsterdam: Elsevier Scientific Publications. 1983.

Juottonen, H., Galand, P. E., Tuittila, E. S., Laine, J., Fritze, H., and Yrjala, K.: Methanogen communities and bacteria along an ecohydrological gradient in a northern raised bog complex. *Environ Microbiol, 7*(10), 1547-1557. doi:10.1111/j.1462-2920.2005.00838.x, 2005.

Juottonen, H., Kotiaho, M., Robinson, D., Merila, P., Fritze, H., and Tuittila, E.S.: Microform-related community patterns of
645 methane-cycling microbes in boreal *Sphagnum* bogs are site specific. *Fems Microbiol Ecol, 91*(9). doi:10.1093/femsec/fiv094, 2015.

Juutinen, S., Väliranta, M., Kuutti, V., Laine, A.M., Virtanen, T., Seppä, H., Weckstrom, J., and Tuittila, E-S.: Short-term and long-term carbon dynamics in a northern peatland-stream-lake continuum: A catchment approach. *J Geophys Res-Biogeo*, 118, 171-183. doi: 10.1002-jgrg.20028, 2013.

650 Juutinen, S., Virtanen, T., Kondratyev, V., Laurila, T., Linkosalmi, M., Mikola, J., Nyman, J., Rasanen, A., Tuovinen, J-P., and Aurela, M.: Spatial variation and seasonal dynamics of leaf-area index in the arctic tundra-implications for linking ground observations and satellite images. *Environ Res Lett, 12*(9). doi:10.1088/1748-9326/aa7f85, 2017.

Kirschke, S., Bousquet, P., Ciais, P., Saunois, M., Canadell, J. G., Dlugokencky, E. J., Bergamaschi, P., Bergmann, D., Blake, D. R., Bruhwiler, L., Cameron-Smith, P., Castaldi, S., Chevallier, F., Feng, L., Fraser, A., Heimann, M.,
655 Hodson, E. L., Houweling, S., Josse, B., Fraser, P. J., Krummel, P. B., Lamarque, J. F., Langenfelds, R. L., Le Quere, C., Naik, V., O'Doherty, S., Palmer, P. I., Pison, I., Plummer, D., Poulter, B., Prinn, R. G., Rigby, M., Ringeval, B., Santini, M., Schmidt, M., Shindell, D. T., Simpson, I. J., Spahni, R., Steele, L. P., Strode, S. A., Sudo, K., Szopa, S., van der Werf, G. R., Voulgarakis, A., van Weele, M., Weiss, R. F., Williams, J. E. and Zeng, G.: Three decades of global methane sources and sinks. *Nat Geosci, 6*(10), 813-823. doi:10.1038/Ngeo1955, 2013.

660 Kokkonen, N. A. K., Laine, A. M., Laine, J., Vasander, H., Kurki, K., Gong, J. N., and Tuittila, E. S.: Responses of peatland vegetation to 15-year water level drawdown as mediated by fertility level. *J Veg Sci, 30*(6), 1206-1216. doi:10.1111/jvs.12794, 2019.

Kolton, M., Marks, A., Wilson, R. M., Chanton, J. P., and Kostka, J. E.: Impact of warming on greenhouse gas production and microbial diversity in anoxic peat from a *Sphagnum*-dominated bog (Grand Rapids, Minnesota, United States).
665 *Front Microbiol, 10*. doi:10.3389/ fmicb.2019.00870, 2019.

Korhola, A., Ruppel, M., Seppä, H., Väliranta, M., Virtanen, T., and Weckström, J.: The importance of northern peatland expansion to the late-Holocene rise of atmospheric methane. *Quaternary Sci Rev, 29*(5-6), 611-617. doi:10.1016/j.quascirev.2009.12.010, 2010.

Korrensalo, A., Männistö, E., Alekseychik, P., Mammarella, I., Rinne, J., Vesala, T., and Tuittila, E.-S.: Small spatial
670 variability in methane emission measured from a wet patterned boreal bog. *Biogeosciences, 15*(6), 1749-1761. doi:10.5194/bg-15-1749-2018, 2018.

Lai, D. Y. F.: Methane dynamics in northern peatlands: a review. *Pedosphere, 19*(4), 409-421. doi:10.1016/S1002-0160(09)00003-4, 2009.

Laine, A. M., Juurola, E., Hajek, T., and Tuittila, E. S. *Sphagnum* growth and ecophysiology during mire succession.
675 *Oecologia, 167*(4), 1115-1125. doi:10.1007/s00442-011-2039-4, 2011.

Laine, A. M., Mäkiranta, P., Laiho, R., Mehtätalo, L., Penttilä, T., Korrensalo, A., Minkkinen, K., Fritze, H., and Tuittila, E-S.: Warming impacts on boreal fen $CO_2$ exchange under wet and dry conditions. *Global Change Biol, 25*(6), 1995-2008. doi:10.1111/gcb.14617, 2019.

Laitinen, J., Rehell, S., Huttunen, A., Tahvanainen, T., Heikkilä, R., and Lindholm, T.: Mire systems in Finland — special
680 view to aapa mires and their water-flow pattern. *Suoseura — Finnish Peatland Society, 56*(1), 1-26. 2007.

Larmola, T., Tuittila, E. S., Tiirola, M., Nykanen, H., Martikainen, P. J., Yrjala, K., Tuomivirta, T., and Fritze, H.: The role of *Sphagnum* mosses in the methane cycling of a boreal mire. *Ecology, 91*(8), 2356-2365. doi:10.1890/09-1343.1, 2010.

685     Lohila, A., Aurela, M., Hatakka, J., Pihlatie, M., Minkkinen, K., Penttila, T., and Laurila, T.: Responses of $N_2O$ fluxes to temperature, water table and N deposition in a northern boreal fen. *Eur J Soil Sci, 61*(5), 651-661. doi:10.1111/j.1365-2389.2010.01265.x, 2010.

Luan, J. W., Wu, J. H., Liu, S. R., Roulet, N., and Wang, M.: Soil nitrogen determines greenhouse gas emissions from northern peatlands under concurrent warming and vegetation shifting. *Commun Biol, 2*. doi:10.1038/s42003-019-0370-1, 2019.

690     MacDonald, G. M., Beilman, D. W., Kremenetski, K. V., Sheng, Y. W., Smith, L. C., and Velichko, A. A.: Rapid early development of circumarctic peatlands and atmospheric $CH_4$ and $CO_2$ variations. *Science, 314*(5797), 285-288. doi:10.1126/science.1131722, 2006.

Macrae, M. L., Devito, K. J., Strack, M., and Waddington, J. M.: Effect of water table drawdown on peatland nutrient dynamics: implications for climate change. *Biogeochemistry, 112*(1-3), 661-676. doi:10.1007/s10533-012-9730-3, 695     2013.

Maechler, M., Rousseeuw, P., Struyf, A., Hubert, M., and Hornik, K. (2019). Cluster Analysis Basics and Extensions.

Mäkiranta, P., Laiho, R., Mehtötalo, L., Strakova, P., Sormunen, J., Minkkinen, K., Penttila, T., Fritze, H., and Tuittila, E-S..: Responses of phenology and biomass production of boreal fens to climate warming under different water-table level regimes. *Global Change Biol, 24*(3), 944-956. doi:10.1111/gcb. 13934, 2018.

700     Mathijssen, P., Tuovinen, J-P., Lohila, A., Aurela, M., Juutinen, S., L, Tuomas., Niemela, E., Tuittila, E-S., and Valiranta, M.: Development, carbon accumulation, and radiative forcing of a subarctic fen over the Holocene. *Holocene, Special issue: Holocene peatland carbon dynamics in the circum-Arctic region*, 1-11. doi:10.1177/0959683614538072, 2014.

Mitchell, C.P.J., and Branfireun, B.A.: Hydrogeomorphic controls on reduction-oxidation conditions across boreal upland-705     peatland interfaces. *Ecosystems*, 8, 731-747. doi:10.1007/s10021-005-1792-9, 2005.

Nijp, J. J., Limpens, J., Metselaar, K., Peichl, M., Nilsson, M. B., van der Zee, S. E. A. T. M., and Berendse, F.: Rain events decrease boreal peatland net $CO_2$ uptake through reduced light availability. *Global Change Biol, 21*(6), 2309-2320. doi:10.1111/gcb.12864, 2015.

Noyce, G. L., Varner, R. K., Bubier, J. L., and Frolking, S.: Effect of *Carex rostrata* on seasonal and interannual variability 710     in peatland methane emissions. *J Geophy Res-Biogeo, 119*(1), 24-34. doi:10.1002/2013jg002474, 2014.

Oquist, M. G., and Svensson, B. H.: Vascular plants as regulators of methane emissions from a subarctic mire ecosystem. *J Geophy Res-Atmos*, *107*(D21). doi:10.1029/2001jd001030, 2002.

Peichl, M., Gazovic, M., Vermeij, I., de Goede, E., Sonnentag, O., Limpens, J., and Nilsson, M. B.: Peatland vegetation composition and phenology drive the seasonal trajectory of maximum gross primary production. *Sci Rep, 8*. 715     doi:10.1038/s41598-018-26147-4, 2018.

Pelletier, L., Moore, T. R., Roulet, N. T., Garneau, M., and Beaulieu-Audy, V.: Methane fluxes from three peatlands in the La Grande Riviere watershed, James Bay lowland, Canada. *J Geophy Res-Biogeo, 112*(G1). doi:10.1029/2006jg000216, 2007.

Peltoniemi, K., Laiho, R., Juottonen, H., Kiikkila, O., Makiranta, P., Minkkinen, K., Pennanen, T., Penttila, T., Sarjala, T., 720     Tuittila, E-S., Tuomivirta, T., and Fritze, H.: Microbial ecology in a future climate: effects of temperature and moisture on microbial communities of two boreal fens. *Fems Microbiol Ecol, 91*(7). doi:10. 1093/femsec/fiv062, 2015.

Pirinen, P., Simola, H., Aalto, J., Kaukoranta, J.-P., Karlsson, P., and Ruuhela, R.: Finnish Meteorological Institute Reports. Tilastoja Suomen Ilmastosta 1981-2010 (Climatological Statistics of Finland 1981-2010), vol. 1. 2012.

725     Radu, D.D., and Duval, T.P.: Impacts of rainfall regime on methane flux from a cool temprate fen depends on vegetation cover. *Ecol Eng*, 114, 76-87. doi: 10.1016/j.ecoleng.20 17.06.047, 2018.

Räsänen, A., Aurela, M., Juutinen, S., Kumpula, T., Lohila, A., Penttilä, T., Virtanen, T.: Detecting northern peatland vegetation patterns at ultra-high spatial resolution. Remote Sens Ecol Con. doi:10.1002/rse2.140, 2020.

Riley, W. J., Subin, Z. M., Lawrence, D. M., Swenson, S. C., Torn, M. S., Meng, L., Mahowald, N. M., and Hess, P.: 730     Barriers to predicting changes in global terrestrial methane fluxes: analyses using CLM4Me, a methane biogeochemistry model integrated in CESM. *Biogeosciences, 8*(7), 1925-1953. doi:10.5194/bg-8-1925-2011, 2011.

Rinne, J., Tuittila, E. S., Peltola, O., Li, X. F., Raivonen, M., Alekseychik, P., Haapanala, S., Pihlatie, M., Aurela, M., Mammarella, I., and Vesala, T.: Temporal variation of ecosystem scale methane emission from a boreal fen in relation to temperature, water table position, and carbon dioxide fluxes. *Global Biogeochem Cy, 32*(7), 1087-1106. 735     doi:10.1029/2017gb005747, 2018.

Riutta, T., Korrensalo, A., Laine, A. M., Laine, J., and Tuittila, E.-S.: Interacting effects of vegetation components and water level on methane dynamics in a boreal fen. *Biogeosciences, 17*(3), 727-740. doi:10.5194/bg-17-727-2020, 2020.

Riutta, T., Laine, J., Aurela, M., Rinne, J., Vesala, T., Laurila, T., Haapanala, S., Pihlatie, M., and Tuittila, E-S.: Spatial variation in plant community functions regulates carbon gas dynamics in a boreal fen ecosystem. *Tellus B, 59*(5),
740      838-852. doi:10.1111/j.1600-0889.2007.00302.x, 2007.

Robroek, B. J. M., Jassey, V. E. J., Kox, M. A. R., Berendsen, R. L., Mills, R. T. E., Cécillon, L., Puissant, J., Meima-Franke, M., Bakker, P. A. H. M., and Bodelier, P. L. E.: Peatland vascular plant functional types affect methane dynamics by altering microbial community structure. *J Ecol, 103*(4), 925-934. doi:10.1111/1365-2745.12413, 2015.

Roulet, N., Moore, T., Bubier, J., and Lafleur, P.: Northern fens: methane flux and climatic change. *Tellus B, 44B*(2), 100-
745      105. 1992.

Rydin, H., and Jeglum, J. K.: *The biology of peatlands*. United Kingdom: Oxford University Press. 2013.

Song, C., Luan, J., Xu, X., Ma, M., Aurela, M., Lohila, A., Mammarella, I., Alekseychik, P., Tuittila, E-S., Gong, W., Chen, X, Meng, X., and Yuan, W.: A microbial functional group-based $CH_4$ model integrated into a terrestrial ecosystem model: model structure, site-level evaluation and sensitivity analysis. *J Adv Model Earth Sy*.
750      doi:10.1029/2019ms001867, 2020.

Strack, M., and Waddington, J. M.: Response of peatland carbon dioxide and methane fluxes to a water table drawdown experiment. *Global Biogeochem Cy, 21*(1). doi:10.1029/2006 gb002715, 2007.

Strack, M., Waddington, J. M., Rochefort, L., and Tuittila, E. S.: Response of vegetation and net ecosystem carbon dioxide exchange at different peatland microforms following water table drawdown. *J Geophy Res-Biogeo, 111*(G2). doi:10.
755      1029/2005jg 000145, 2006.

Strack, M., Waddington, J. M., and Tuittila, E.-S.: Effect of water table drawdown on northern peatland methane dynamics: Implications for climate change. *Global Biogeochem Cy, 18*(4). doi:10.1029/2003gb002209, 2004.

Strakova, P., Penttila, T., Laine, J., and Laiho, R.: Disentangling direct and indirect effects of water table drawdown on above- and belowground plant litter decomposition: consequences for accumulation of organic matter in boreal
760      peatlands. *Global Change Biol, 18*(1), 322-335. doi:10.1111/j.1365-2486.2011.02503.x, 2012.

Ström, L., Ekberg, A., Mastepanov, M., and Christensen, T. R.: The effect of vascular plants on carbon turnover and methane emissions from a tundra wetland. *Global Change Biol, 9*(8), 1185-1192. doi:10.1046/j.1365-2486.2003.00655.x, 2003.

Tuittila, E.-S., Väliranta, M., Laine, J., and Korhola, A.: Quantifying patterns and controls of mire vegetation succession in a
765      southern boreal bog in Finland using partial ordinations. *J Veg Sci, 18*, 891-902. 2007.

Turetsky, M. R., Crow, S. E., Evans, R. J., Vitt, D. H., and Wieder, R. K.: Trade-offs in resource allocation among moss species control decomposition in boreal peatlands. *J Ecol, 96*(6), 1297-1305. doi:10.1111/j.1365-2745.2008.01438.x, 2008.

Turetsky, M. R., Kotowska, A., Bubier, J., Dise, N. B., Crill, P., Hornibrook, E. R. C., Minkkinen, K., Moore, T.R., Myers-
770      Smith, I.H., Nykanen, H., Olefeldt, D., Rinne, J., Saarnio, S., Shurpali, N., Tuittila, E-S., Waddington, J.M., White, J.R., Wickland, K.P., and Wilmking, M.: A synthesis of methane emissions from 71 northern, temperate, and subtropical wetlands. *Global Change Biol, 20*(7), 2183-2197. doi:10.1111/gcb.12580, 2014.

Turetsky, M. R., Treat, C. C., Waldrop, M. P., Waddington, J. M., Harden, J. W., and McGuire, A. D.: Short-term response of methane fluxes and methanogen activity to water table and soil warming manipulations in an Alaskan peatland. *J*
775      *Geophy Res-Biogeo, 113*. doi:10.1029/2007jg000496, 2008.

Oksanen, J., Blanchet, F.G., Friendly, M., Kindt, R., Legendre, P., McGlinn, D., et al.: vegan: Community Ecology Package. *R package version 2.5-6*. 2019

Wassen, M. J., Barendregt, A., Palczynski, A., Desmidt, J. T., and Demars, H.: The relationship between fen vegetation gradients, groundwater-flow and flooding in an undrained valley mire at Biebrza, Poland. *J Ecol, 78*(4), 1106-1122.
780      doi:10.2307/2260955, 1990.

Weltzin, J. F., Pastor, J., Harth, C., Bridgham, S. D., Updegraff, K., and Chapin, C. T.: Response of bog and fen plant communities to warming and water-table manipulations. *Ecology, 81*(12), 3464-3478. doi:10.1890/0012-9658(2000)081[3464:Robafp]2.0.Co;2, 2000.

Wheeler, B. D., and Proctor, M. C. F.: Ecological gradients, subdivisions and terminology of north-west European mires. *J*
785      *Ecol, 88*(2), 187-203. doi:10.1046/j.1365-2745.2000. 00455.x, 2000.

Whiting, G. J., and Chanton, J. P.: Primary production control of methane emission from wetlands. *Nature, 364*(6440), 794-795. doi:10.1038/364794a0, 1993.

31

Wu, J., Kutzbach, L., Jager, D., Wille, C., and Wilmking, M.: Evapotranspiration dynamics in a boreal peatland and its impact on the water and energy balance. *J Geophy Res, 115*, doi:10.1029/2009JG001075, 2010.

790    Yavitt, J. B., Kryczka, A. K., Huber, M. E., Pipes, G. T., and Rodriguez, A. M.: Inferring methane production by decomposing tree, shrub, and grass leaf litter in bog and rich fen peatlands. *Front Environ Sci, 7.* doi:10.3389/fenvs.2019.00182, 2019.

Yrjälä, K. I. M., Tuomivirta, T., Juottonen, H., Putkinen, A., Lappi, K., Tuittila, E.-S., Penttila, T., Minkkinen, K., Laine, J., Peltoniemi, K., and Fritze, H.: $CH_4$ production and oxidation processes in a boreal fen ecosystem after long-term

795    water table drawdown. *Global Change Biol, 17*(3), 1311-1320. doi:10.1111/j.1365-2486.2010.02290.x, 2011.

Zhang, H., Piilo, S. R., Amesbury, M. J., Charman, D. J., Gallego-Sala, A. V., and Väliranta, M. M.: The role of climate change in regulating Arctic permafrost peatland hydrological and vegetation change over the last millennium. *Quaternary Sci Rev, 182*, 121-130. doi:10.1016/j.quascirev.2018.01.003, 2018.

Zhang, Y., Li, C. S., Trettin, C. C., Li, H., and Sun, G.: An integrated model of soil, hydrology, and vegetation for carbon

800    dynamics in wetland ecosystems. *Global Biogeochem Cy, 16*(4). doi:10.1029/2001gb001838, 2002.

Zhang, Z., Zimmermann, N. E., Stenke, A., Li, X., Hodson, E. L., Zhu, G. F., Huang, C.L., and Poulter, B.: Emerging role of wetland methane emissions in driving 21st century climate change. *P Nati Acad Sci USA, 114*(36), 9647-9652. doi:10.1073/pnas.1618765114, 2017.